

## Utility of deep sea CO<sub>2</sub> release experiments in understanding the biology of a high-CO<sub>2</sub> ocean: Effects of hypercapnia on deep sea meiofauna

James P. Barry, Kurt R. Buck, Chris Lovera, Linda Kuhnz, and Patrick J. Whaling  
Monterey Bay Aquarium Research Institute, Moss Landing, California, USA

Received 26 July 2004; revised 21 February 2005; accepted 29 April 2005; published 9 September 2005.

[1] Oceanic CO<sub>2</sub> levels are expected to rise during the next 2 centuries to levels not seen for 10–150 million years by the uptake of atmospheric CO<sub>2</sub> in surface waters or potentially through the disposal of waste CO<sub>2</sub> in the deep sea. Changes in ocean chemistry caused by CO<sub>2</sub> influx may have broad impacts on ocean ecosystems. Physiological processes animals use to cope with CO<sub>2</sub>-related stress are known, but the range of sensitivities and effects of changes in ocean chemistry on most ocean life remain unclear. We evaluate the effectiveness of various designs for in situ CO<sub>2</sub> release experiments in producing stable perturbations in seawater chemistry over experimental seafloor plots, as is desirable for evaluating the CO<sub>2</sub> sensitivities of deep sea animals. We also discuss results from a subset of these experiments on the impacts of hypercapnia on deep sea meiofauna, in the context of experimental designs. Five experiments off central California show that pH perturbations were greatest for experiments using “point source” CO<sub>2</sub> pools surrounded by experimental plots. CO<sub>2</sub> enclosure experiments with experimental plots positioned within a circular arrangement of CO<sub>2</sub> pools had more moderate pH variation. The concentration of dissolution plumes from CO<sub>2</sub> pools were related to the speed and turbulence of near-bottom currents, which influence CO<sub>2</sub> dissolution and advection. Survival of meiofauna (nematodes, amoebae, euglenoid flagellates) was low after episodic severe hypercapnia but lower and variable where pH changes ranged from 0 to 0.2 pH units below normal.

**Citation:** Barry, J. P., K. R. Buck, C. Lovera, L. Kuhnz, and P. J. Whaling (2005), Utility of deep sea CO<sub>2</sub> release experiments in understanding the biology of a high-CO<sub>2</sub> ocean: Effects of hypercapnia on deep sea meiofauna, *J. Geophys. Res.*, *110*, C09S12, doi:10.1029/2004JC002629.

### 1. Introduction

[2] The chemistry of the world ocean is changing rapidly due to the influx of anthropogenic carbon dioxide from the atmosphere. This process will almost certainly intensify in the near future as CO<sub>2</sub> emissions increase, with potentially profound impacts on the structure and function of ocean ecosystems. Since the onset of the industrial revolution, the oceans have absorbed ~118 Pg of anthropogenic carbon, or roughly 48% of the total carbon emissions [Sabine *et al.*, 2004]. Present carbon emissions near 7 PgC yr<sup>-1</sup> are expected to increase to 15 PgC yr<sup>-1</sup> by 2050 [Marland *et al.*, 2001] (available at <http://cdiac.esd.ornl.gov/trends/trends.htm>) and potentially to over 20 PgC yr<sup>-1</sup> by the end of this century [Joos *et al.*, 1999; Leggett *et al.*, 1992]. Equilibration of ocean waters with the atmosphere has already acidified ocean surface waters by 0.1 pH units [Haugan and Drange, 1992] and ocean mixing, though slow, has allowed anthropogenic carbon to penetrate to 1000+ m over much of the ocean [Sabine *et al.*, 2004].

Continued acidification will reduce ocean pH by an additional 0.2 units by the end of this century [Haugan and Drange, 1992], and the accumulating atmospheric burden of carbon dioxide is expected to reach 1900 ppm during the next 200–300 years, leading to pH reduction of 0.7 units in ocean surface waters, levels nonexistent on Earth for over 300 million years [Caldeira and Wickett, 2003].

[3] The ecosystem consequences of elevated atmospheric CO<sub>2</sub> are large. The increase of 0.75°C in global temperature over the last century is considered by many scientists to have been driven by CO<sub>2</sub>-related greenhouse warming, and is associated with broad changes in marine and terrestrial ecosystems [Parmesan and Yohe, 2003; Root *et al.*, 2003]. In addition to warming effects, acidification and the reduced carbonate saturation state of the oceans has now been implicated in reduced rates of calcification of many carbonate secreting marine taxa, ranging from microscopic plankton to coral reefs [Feely *et al.*, 2004].

[4] Efforts to stabilize atmospheric greenhouse gas levels or at least mitigate the effects of accelerating carbon dioxide emissions have led to several carbon management options including carbon sequestration in the terrestrial biosphere, the world ocean, and acceptable geological strata. Options

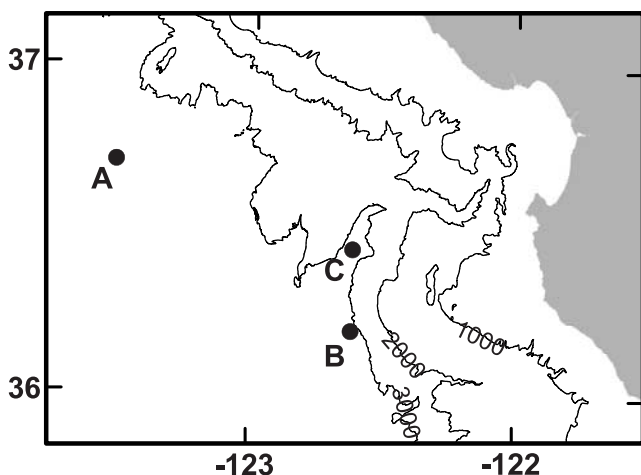


**Figure 1.** Map of sites for CO<sub>2</sub> release experiments off central California.

for ocean carbon storage have focused on direct deep sea CO<sub>2</sub> injection or indirect deep sea storage by enhancing the natural carbon flux to the deep sea via fertilization of ocean surface waters with micronutrients [Martin, 1990]. Although direct ocean sequestration of CO<sub>2</sub> was suggested 25 years ago [Marchetti, 1977], it has recently received more interest, due to greater awareness of climate trends and political attention to national energy policies [Kerr, 2001].

[5] Our understanding of the biological and ecological consequences of large changes in the carbonate chemistry of the oceans is poor, for both shallow and deep ocean ecosystems, and has received considerably less attention than terrestrial systems, where large-scale studies to measure the response of ecosystems to elevated CO<sub>2</sub> levels are ongoing [e.g., McLeod and Long, 1999] (available at <http://cdiac.esd.ornl.gov>). Recent sophisticated mesocosm studies of marine plankton communities [Riebesell et al., 2000] and coral reef systems [Langdon et al., 2003] have advanced our understanding of increased carbon dioxide levels on some surface ocean systems. However, a considerable increase in research is required to generate a comprehensive understanding of the response of marine organisms to changes in ocean chemistry caused by either the continuing invasion of carbon dioxide into surface waters or CO<sub>2</sub> sequestration in the deep sea. Experiments to examine the effects of hypercapnia on deep sea biota are an important step in advancing our understanding of the high-CO<sub>2</sub> ocean that is almost certain in Earth's future.

[6] We performed a series of deep sea CO<sub>2</sub> release experiments to investigate the effects of hypercapnia on deep sea biota, as might be expected to result from a direct ocean carbon sequestration program, by potential leakage into deep ocean water of CO<sub>2</sub> injected into geologic formations under the seabed, or eventually by the chronic elevation of seawater chemistry due to air-sea exchange and deep ocean mixing. Although seawater chemistry near CO<sub>2</sub> release sites of any large-scale CO<sub>2</sub> sequestration program will vary greatly depending on the rates and methods of release and the stirring and mixing rates of the near-bottom physical processes [Shirayama, 1998], long-term (i.e., centuries), large-scale (ocean basin) changes in total CO<sub>2</sub> and

pH of the deep ocean will probably be less variable in space and time, with changes in ocean pH dependent upon CO<sub>2</sub> injection volumes and retention efficiency [Harvey, 2003]. Our CO<sub>2</sub> release experiments were intended to produce quasi-stable, month-long perturbations of the CO<sub>2</sub> content of waters overlying experimental plots on the seafloor through their exposure to the hypercapnic dissolution plume advected from adjacent seafloor pools of liquid CO<sub>2</sub>. The severity of hypercapnia and pH disturbance was intended to approach values expected from either the regional effects of a direct deep sea CO<sub>2</sub> sequestration program or from the chronic acidification of the ocean by atmospheric CO<sub>2</sub> influx. In this paper we examine the efficacy of various experimental designs for CO<sub>2</sub> release experiments in providing stable perturbations to the CO<sub>2</sub> and pH content of seawater bathing experimental plots. In addition to our focus on the efficiency of these methods, we discuss a subset of the results from these experiments concerning the effects of hypercapnia on deep sea meiofauna.

## 2. Methods

### 2.1. Study Area

[7] CO<sub>2</sub> release experiments were conducted at three locations on the continental rise in 3250–3600 m depth off the coast of central California (Figure 1). The abyssal seafloor at sites A and B is flat and relatively featureless, covered with fine-grained clay-rich sediment with a high content of organic carbon (~3% dry wt). Bottom water at these sites is cold (1.5°–1.6°C), with oxygen levels of 120 μM, alkalinity of 2440 μm kg<sup>-1</sup>, in situ pH of ~7.78 (SWS) and total CO<sub>2</sub> of 2350 μm kg<sup>-1</sup>. Site C is located in the axis of lower Monterey Canyon, a large submarine canyon extending from the shore to >4000 m depth. This section of Monterey Canyon is wide (~2 km), and relatively flat, with fine-grained surficial sediments. Studies at all sites were at depths well below the intense oxygen minimum typical of eastern Pacific waters, where oxygen stress could compound the effects of hypercapnia alone on deep sea organisms [Pörtner et al., 2005].

[8] Benthic and benthopelagic megafauna are common, but distributed sparsely at the study sites. The sediment-dwelling infauna at most sites was dominated by crustaceans, especially tube-dwelling ampeliscid amphipods, and polychaeta worms. Benthic meiofauna, the focus of this paper, were dominated by nematode worms, euglenoid flagellates, amoebae, ciliates, and allogromiid foraminifera.

### 2.2. Carbon Dioxide Release Experiments

[9] Several CO<sub>2</sub> release experiments were performed from 2001 to 2003 off central California at depths of 3100–3600 m (Table 1). The installation, sampling, and recovery of CO<sub>2</sub> experiments were performed using the ROV *Tiburón*, launched from the R/V *Western Flyer*, and operated by the Monterey Bay Aquarium Research Institute (MBARI). Details concerning the R/V *Tiburón* are available at <http://www.mbari.org>. A remotely operated vehicle (ROV)-mounted CO<sub>2</sub> release system developed by MBARI was used to dispense up to 40 L of liquid CO<sub>2</sub> per ROV dive. This system was nearly identical to the CO<sub>2</sub> release system described by Brewer et al. [1999], but had a capacity of 40 L. For each approximately month-long experiment,

**Table 1.** List of CO<sub>2</sub> Release Experiments

Experiment	Design	Site	Latitude, deg	Longitude, deg	Depth, m	Start Date	Duration, days
CO <sub>2</sub> -1	point source	A	36.709	-123.523	3600	25 Jun 2001	36
CO <sub>2</sub> -2	point source	B	36.200	-122.617	3310	25 Oct 2001	41
CO <sub>2</sub> -3	point source	A	36.708	-123.531	3650	4 Apr 2002	27
CO <sub>2</sub> -4	CO <sub>2</sub> enclosure	C	36.378	-122.676	3262	11 Nov 2002	29
CO <sub>2</sub> -5	CO <sub>2</sub> enclosure	A	36.709	-123.523	3607	19 Aug 2003	31

we released liquid CO<sub>2</sub> into small “corrals” (sections of PVC pipe ~40–100 cm in diameter × 12–40 cm high) placed on the seafloor, creating small, contained pools of liquid CO<sub>2</sub> (Figure 2). Upon its release into corrals, liquid CO<sub>2</sub> dissolved slowly, producing a CO<sub>2</sub>-rich, low-pH dissolution plume that was advected and dispersed downstream by near-bottom currents. The CO<sub>2</sub> dissolution plume becomes negatively buoyant as CO<sub>2</sub> hydration occurs [Brewer *et al.*, 2005], and thus, flows as a dense plume relative to seawater, interacting with the surficial sediments. Because of the difficulties of measuring seawater CO<sub>2</sub> in situ, we measured variation in pH caused by the CO<sub>2</sub> dissolution plume as a proxy for its CO<sub>2</sub> content. The intensity and variability of CO<sub>2</sub> dissolution plumes were measured just above the seafloor using pH electrodes installed on conductivity-temperature-depth (CTD) sensors.

[10] Depths greater than 3000 m were selected for CO<sub>2</sub> injection experiments for several reasons. Large-scale carbon sequestration by direct ocean injection will likely target abyssal depths due to the greater storage efficiency of CO<sub>2</sub> injections at these depths, compared to shallow injection scenarios [Herzog *et al.*, 2001]. Therefore research on the sensitivities of bathyal and abyssal deep sea biota to changes in seawater chemistry caused by CO<sub>2</sub> injection is required to assess the ecosystem consequences of any ocean carbon sequestration scenario. In addition, the phase stability characteristics of CO<sub>2</sub> are such that liquid CO<sub>2</sub> is positively buoyant to a depth of ~2600 m off central California. CO<sub>2</sub> released at 3200–3600 m has a density of 1.064–1.074 kg L<sup>-1</sup> (E. Peltzer, unpublished data, 2004). Because CO<sub>2</sub> is denser than seawater at depths greater than 2600 m, we were able to release liquid CO<sub>2</sub> into PVC corrals placed on the seafloor. At shallower depths, the liquid CO<sub>2</sub> would float toward the surface and dissolve or undergo a phase change to a gaseous state (~340 m depth), making these experiments less tractable or impossible.

[11] The effect of hypercapnia on benthic meiofauna (flagellates, amoebae, nematodes) inhabiting the surficial (i.e., top 1 cm) sediments was examined in these experiments by assessing their survival (estimated from changes in abundance) in experimental plots near and distant from CO<sub>2</sub> pools, related to the severity of hypercapnia. Because meiofauna inhabit the sediment, the key measurements of interest are the pH and CO<sub>2</sub> content of pore fluids relative to ambient values. While limited pH profiles of the sediments were performed during one experiment [Thistle *et al.*, 2005], these measurements were only possible at the beginning or end of the experiments, and thus, could not track the temporal sequence of pore fluid perturbations by the dissolution plume. In view of this limitation, we assumed that pore fluids in top 1 cm of the sediment also became hypercapnic due to the CO<sub>2</sub> dissolution plume, as shown by

[Thistle *et al.*, 2005]. It is expected that the temporal variability of hypercapnia observed in bottom water (see below) was smoothed somewhat in the upper sediment layer, but was representative of changes in the pH field measured ~3 cm above the seafloor.

[12] Five CO<sub>2</sub> release experiments with differing configurations of CO<sub>2</sub> pools and seafloor study plots were performed (Figure 3), among which the intensity and stability of hypercapnia were expected to vary (Table 1). These ranged from point source CO<sub>2</sub> designs, where pools of liquid CO<sub>2</sub> were surrounded by experimental plots containing organisms (Figures 3a and 3b), to layouts where plots were encircled by multiple CO<sub>2</sub> corrals (CO<sub>2</sub> enclosure designs (Figures 3c and 3d)). These latter designs, similar in configuration to terrestrial Free-Air CO<sub>2</sub> Enrichment (FACE) experimental designs [Allen, 1992a, 1992b; Allen and Beladi, 1990] were expected to produce the most stable pH and CO<sub>2</sub> perturbations.

### 2.3. Point Source CO<sub>2</sub> Pool Experiments

#### 2.3.1. CO<sub>2</sub>-1: Replicated Acute CO<sub>2</sub> Exposure Design

[13] This initial experiment to examine in situ the response of abyssal deep sea biota to hypercapnic conditions was designed as an ANOVA comparison of the survival of animals between replicated CO<sub>2</sub> and control treatments. Details of the experimental design and results concerning the impacts on benthic meiofauna are presented by Barry *et al.* [2004]. We provide a brief overview of that experiment here. Six small (48 cm diameter × 15 cm high) PVC corrals were placed on the seafloor (Figure 3a) at 3600 m depth at site A (Figure 1). Three of the six corrals were each filled with ~20 L of reagent-grade liquid CO<sub>2</sub> (Figures 2a and 2b) using the MBARI CO<sub>2</sub> delivery system, refilled after 14 days, and the experiment was terminated after a total of 36 days (Table 1).

[14] Seawater chemistry near these pools was measured using three CTDs equipped with pH sensors, positioned ~3 cm above the seafloor and near (<0.5 m) two of the CO<sub>2</sub>-filled corrals (e.g., Figure 2a, upper left) and one of the control corrals. Current patterns at the site were measured with an upward-looking acoustic Doppler current profiler (ADCP) positioned 2 m above the seafloor on a small mooring located ~70 from the experimental pools.

[15] Tolerance to hypercapnia by sediment-dwelling meiofauna was examined by comparing the abundances of live meiofaunal taxa near CO<sub>2</sub> and control corrals, at the beginning of the study prior to dispensing liquid CO<sub>2</sub> and at the end of the experiment 36 days later (Table 1). Sediments were sampled from replicate sediment cores (MBARI tube cores: 7 cm diameters × 15–20 cm deep) collected adjacent to, i.e., <0.5 m from, CO<sub>2</sub> and control corrals.

[16] Meiofaunal abundance was quantified by extracting the top 1 cm of sediment from a subsample of each core

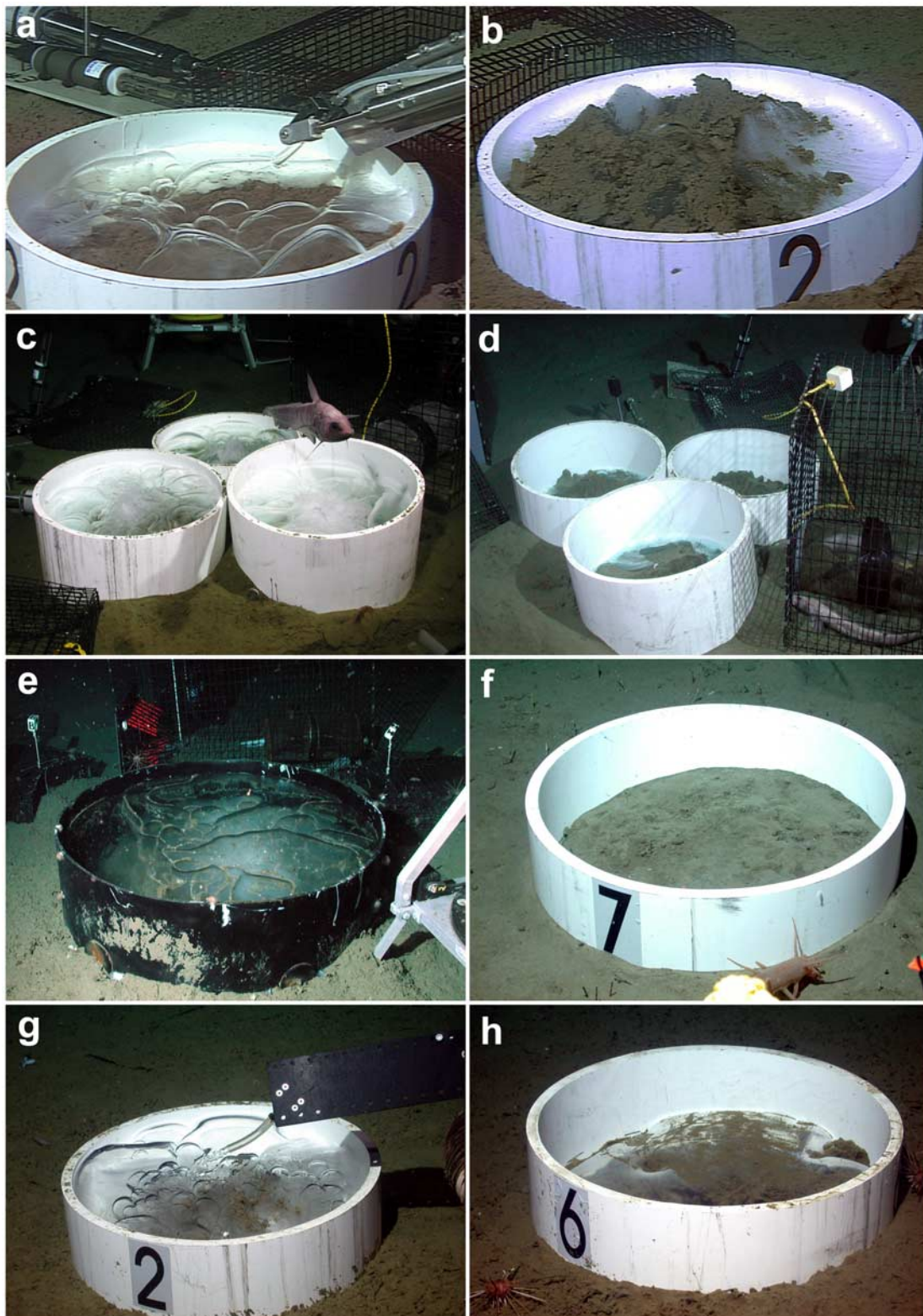


**Figure 2.** CO<sub>2</sub> corral during CO<sub>2</sub> release experiments. (a) Initial filling of corral 2 during CO<sub>2</sub>-1. Note pH sensor in upper left. (b) “Frost heave” of sediment in CO<sub>2</sub>-1 corral 2 (Figure 2a) after 1 day, caused by interaction of CO<sub>2</sub> hydrate with sediment. (c) Full central CO<sub>2</sub> corral (~100 L liquid CO<sub>2</sub>) at beginning of CO<sub>2</sub>-2. Macrourid fish is swimming above CO<sub>2</sub>. (d) Central corral after 49 days dissolution during CO<sub>2</sub>-2. Note small amount of CO<sub>2</sub> hydrate in bottom and live abyssal zoarcid fish (*Pachycara* sp.) in cage at lower right. (e) Nearly 75% full CO<sub>2</sub> corral with liquid CO<sub>2</sub> and unknown amount of CO<sub>2</sub> hydrate at the end of CO<sub>2</sub>-3. (f) Empty CO<sub>2</sub> corral after 1 month at end of CO<sub>2</sub>-4. (g) Full CO<sub>2</sub> corral at beginning of CO<sub>2</sub>-5. (h) Partially full corral at end of experiment CO<sub>2</sub>-5.

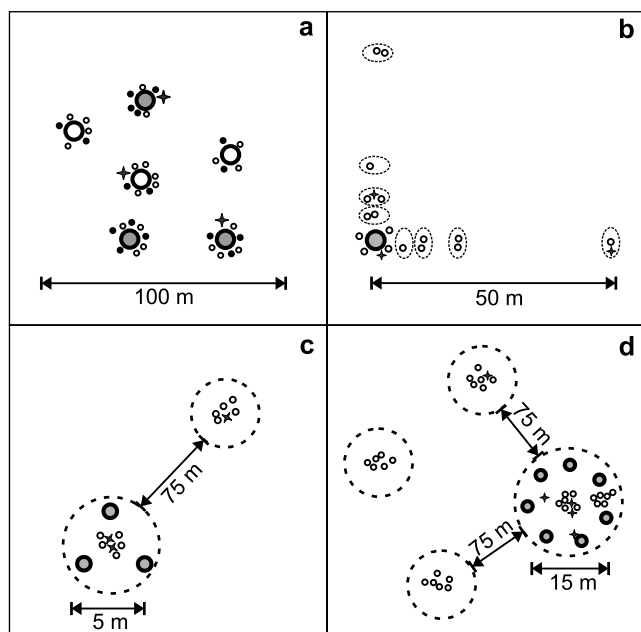


**Figure 3.** Experimental design of CO<sub>2</sub> release experiments. (top) Point source CO<sub>2</sub> release experiments. (bottom) CO<sub>2</sub>-enclosure designs. (a) CO<sub>2</sub>-1, with three randomly distributed CO<sub>2</sub> corrals with ~20 L of liquid CO<sub>2</sub> (large shaded circles) and three unfilled control corrals (open circles). Small circles indicate locations of sediment cores for collection of benthic meiofauna (black, samples prior to CO<sub>2</sub> release; white, samples at end of experiment). Star symbols indicate positions of pH sensors. (b) CO<sub>2</sub> pool layout used for release experiments CO<sub>2</sub>-2 and CO<sub>2</sub>-3. A single central CO<sub>2</sub> corral (~160 L), as used in CO<sub>2</sub>-3, is shown. Triplicate smaller corrals (~100 L total) used in CO<sub>2</sub>-2 not shown. Sediment samples were collected from distances of 1–50 m (indicated by dashed ellipses) from the CO<sub>2</sub> pool in two orthogonal directions. (c) Triangular CO<sub>2</sub> enclosure experiment CO<sub>2</sub>-4 with three ~20 L CO<sub>2</sub> corrals. Dashed circles indicate general area of treatment (CO<sub>2</sub>) and control samples. Control location was ~75 m from CO<sub>2</sub> pool area. (d) Circular CO<sub>2</sub> enclosure experiment CO<sub>2</sub>-5. Symbols as above. Note the seven ~20 L CO<sub>2</sub> corrals.

using a 60 cc syringe with the Luer end removed. Subsamples were preserved immediately in a 2% glutaraldehyde solution in 0.1 M cacodylate buffered, filtered seawater. A Percoll density-gradient centrifugation technique was used to extract meiofauna from aliquots of the subsampled sediment. Counts and biovolume measurements of meiofauna stained with the fluorochrome DAPI were made using epifluorescence microscopy. Details of these techniques are presented by *Buck et al.* [2000]. Tissue condition (live/dead) was assessed for a subsample of nematodes collected. Individual nematodes stained with DAPI were inspected under epifluorescence microscopy for the presence (recently live) or absence (dead) of intact cell nuclei.

### 2.3.2. CO<sub>2</sub>-2, CO<sub>2</sub>-3: CO<sub>2</sub> Exposure Gradient Experiments

[17] We performed two CO<sub>2</sub> release experiments (CO<sub>2</sub>-2, CO<sub>2</sub>-3) using a regression design, by creating relatively

large CO<sub>2</sub> pools in a single, central location, then characterizing the dissolution plume and assessing meiofaunal abundance at distances of 0.5–50 m in two directions (Figure 3b). Considering the acute CO<sub>2</sub> perturbations observed in close proximity to CO<sub>2</sub> pools (see results for CO<sub>2</sub>-1 below), we expected more moderate pH changes (0.1–0.3 units) at distances of ~5–10 m from central CO<sub>2</sub> pools, due to diffusion and mixing of the dissolution plume.

[18] For CO<sub>2</sub>-2 at site B (Figure 1, Table 1), we placed three PVC corrals (48 cm diameter × 40 cm high) in a tight group on the seafloor, filling them with ~100 L of liquid CO<sub>2</sub> (Figures 2c and 2d). Together, they formed a central point source for the hypercapnic dissolution plume. Seabird pH electrodes attached to Applied Microsystems Ltd (AML) CTDs were positioned distances of ~0.5, 5, and 50 m from the CO<sub>2</sub> pools to measure the magnitude of pH (thus CO<sub>2</sub>) perturbations (Figure 3b). An acoustic Doppler current profiler (ADCP) meter mooring was deployed at the site as described for CO<sub>2</sub>-1. The corrals were not refilled during the experiment, which was terminated after 41 days (Table 1). Sediment samples for meiofaunal analyses in each experiment were collected from 0.5, 2, 5, 10, and 50 m to the north and east of the central CO<sub>2</sub> pools at the end of the experiment.

[19] Release experiment CO<sub>2</sub>-3 (site A (Figure 1)) had a similar design (Figure 3b), but used a 91 cm diameter × 30 cm high plastic corral, which was filled with ~75 L of liquid CO<sub>2</sub> at the beginning of the experiment (Figures 2e and 4b), leaving the corral approximately 35% full. Sensors were positioned from 0.5 to 50 m from the CO<sub>2</sub> source as in CO<sub>2</sub>-2. Additional liquid CO<sub>2</sub> (80 L) was added to the corral after 13 days to bring it to ~75% full, and the experiment was terminated after 27 days (Table 1). Sediment samples were collected for meiofaunal analyses as in CO<sub>2</sub>-2.

[20] We estimated the rate of survival for major meiofaunal taxa at the end of each experiment from changes in their biovolume along the exposure gradient, i.e., from 50 to

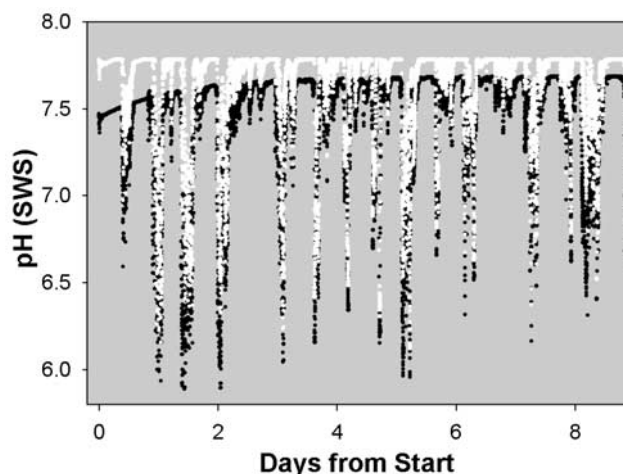


**Figure 4.** Adjustment of raw pH data. Raw data (black dots) were adjusted (white dots) to remove sensor drift, and the baseline pH was offset to match the ambient pH (7.78 SWS).

0.5 m from the CO<sub>2</sub>. Mean meiofaunal biovolume 50 m from CO<sub>2</sub> pools was assumed to represent background (i.e., 100% survival) values, with lower biovolume nearer CO<sub>2</sub> pools reflecting reduced survival. A power function (biovolume =  $a(\text{distance})^b$ ) was fit to the biovolume and distance data set for each meiofaunal taxon to characterize its “survival” versus distance relationship. Several interacting factors affect the dispersion of the dissolution plume and the taxon-specific responses of meiofaunal populations. Complex physical processes such as CO<sub>2</sub> hydration kinetics, dissolution plume density, diffusion, advection, and eddy turbulence will affect the intensity of hypercapnia and acidosis with distance from CO<sub>2</sub> pools. Changes in the biovolume of specific taxa during these experiments represent the integrated effects of individual and numerical population responses to hypercapnic stress. The power function is expected to represent a first-order approximation of the combined effects of physical and biological processes on the dispersal of the dissolution plume and the sensitivity and response of meiofaunal taxa.

## 2.4. CO<sub>2</sub> Enclosure Designs

### 2.4.1. CO<sub>2</sub>-4: Triangular CO<sub>2</sub> Enclosure Design

[21] Release experiment CO<sub>2</sub>-4 was performed using a CO<sub>2</sub> enclosure design in Monterey Canyon at site C (Figure 1, Table 1). Rather than a single-point CO<sub>2</sub> source surrounded by sensors and experimental plots, we designed a triangular CO<sub>2</sub> enclosure in which three CO<sub>2</sub>-filled corrals (48 cm diameter × 15 cm high; ~20 L each) were positioned ~4 m apart at the apices of a roughly equilateral triangle (Figure 3c). Sensors were positioned near the center of the triangular CO<sub>2</sub> corral layout, and sediment samples for meiofaunal analyses were collected from the center of the triangle, and ~75 m from the CO<sub>2</sub> enclosure. An ADCP was moored nearby to measure the flow field, positioned ~16 m above the seafloor and in a downward looking configuration. Meiofauna were enumerated from the upper 1–5 cm of sediments sieved through a 63 μm filter [Carman *et al.*, 2004]. CO<sub>2</sub> was dispensed into all three CO<sub>2</sub> corrals, and the experiment was terminated after 29 days (Table 1).

### 2.4.2. CO<sub>2</sub>-5: Circular CO<sub>2</sub> Enclosure

[22] A CO<sub>2</sub> release experiment performed during 2003 at site A (Figure 1) employed a circular layout of CO<sub>2</sub> corrals (Table 1, Figure 3d) that mimics the concept of terrestrial FACE experiments [McLeod and Long, 1999]. Perturbations to pH and CO<sub>2</sub> within the enclosure design were expected to be more stable than produced using point source designs. Seven CO<sub>2</sub> corrals (48 cm diameter × 15 cm high; ~20 L liquid CO<sub>2</sub> each (Figures 2g and 2h)) were positioned in a circle ~12–15 m in diameter. This size of the enclosure was selected using results of earlier experiments and targeting a ~0.2–0.3 unit pH reduction inside the circle.

[23] CTDs equipped with pH sensors were positioned near the margin of the circle adjacent to a CO<sub>2</sub> corral, ~1.5 m from the margin, and in the center of the circle, as well as in a control area ~75 m distant. Sensors were positioned from 3 to 50 cm above the seafloor.

[24] Sediment cores for meiofaunal studies were collected both before CO<sub>2</sub> injection and at the termination of the month-long experiment, from the center of the CO<sub>2</sub> enclosure, as well as from three nearby (~75 m distance) control

areas. Meiofaunal abundances from this experiment are not yet available and will not be discussed further.

### 2.4.3. Current Measurements

[25] Near-bottom currents were measured during each CO<sub>2</sub> release experiment using an ADCP. The ADCP (RDI sentinel, 300 or 600 kHz) was generally mounted on a small mooring 2 m (CO<sub>2</sub>-1, -2, -3), or 3 m (CO<sub>2</sub>-5) above the seafloor, oriented upward. For CO<sub>2</sub>-4, the ADCP was mounted 16 m above the seafloor, oriented downward. Time series data from a single measurement bin 8 m above the seafloor were used to characterize the flow patterns (mean speeds, progressive vector plots) and for spectral analyses (FFT; Matlab release 14, 2004). Vertical profiles of mean flow speed and eddy turbulence were calculated using all available ADCP data.

### 2.4.4. pH Measurements

[26] Seawater pH was measured using Seabird SBE 18 pH sensors attached to Seabird Model 19 plus or Applied Microsystems Ltd. CTDs. Sensors were mounted from 3 to 50 cm above the bottom, at varying distances from CO<sub>2</sub> pools, depending upon experimental layout. Data intervals varied among experiments from 1 to 6 min.

[27] Frequent failure or drift of deep-rated pH sensors complicated the interpretation of the pH field near CO<sub>2</sub> release experiments. Raw pH data were adjusted to remove sensor drift. Because we were interested primarily in excursions of pH from the average in situ values (assumed constant during each experiment), data from each pH sensor was adjusted such that its maximum values equaled the in situ bottom water pH for that location (normally near 7.78 SWS). Adjusted pH data were calculated as the in situ bottom water pH (7.78) minus the deviation for each measured pH datum from the local (within 12 hours) median or maximum pH (Figure 4).

[28] Spectral analyses of pH records were performed on adjusted data series following Fourier transformation (FFT; Matlab Release 14, 2004).

## 3. Results

### 3.1. Benthic Boundary Layer Currents

[29] The speed and direction of deep sea currents during all CO<sub>2</sub> release experiments varied in time and among experiments, affecting both the rate of dissolution and advection of the dissolution plume from experimental CO<sub>2</sub> pools. Currents 8 m above the seabed were generally sluggish (mean speed ~3–6 cm/s) and oscillatory in speed and direction during all release experiments (Figure 5), and were dominated by tidal and, to a lesser degree, inertial motions. A summary of current data from 8 m above the seafloor, the depth nearest the seafloor where data are available from each experiment (no data are available from CO<sub>2</sub>-3), is presented in Table 2.

[30] Although flow during all experiments was rotary to some degree, the key differences in flow among experiments related to the average speed and turbulence of flow near the bottom (Figure 6), which influence both the dissolution of liquid CO<sub>2</sub> and the dispersal and mixing of the plume. Highest mean absolute and net flow speeds were measured during CO<sub>2</sub>-4 at site C where flow is constrained bathymetrically by the walls of Monterey Canyon (Table 2). Mean current speed was higher (5.7 cm s<sup>-1</sup>) than measured

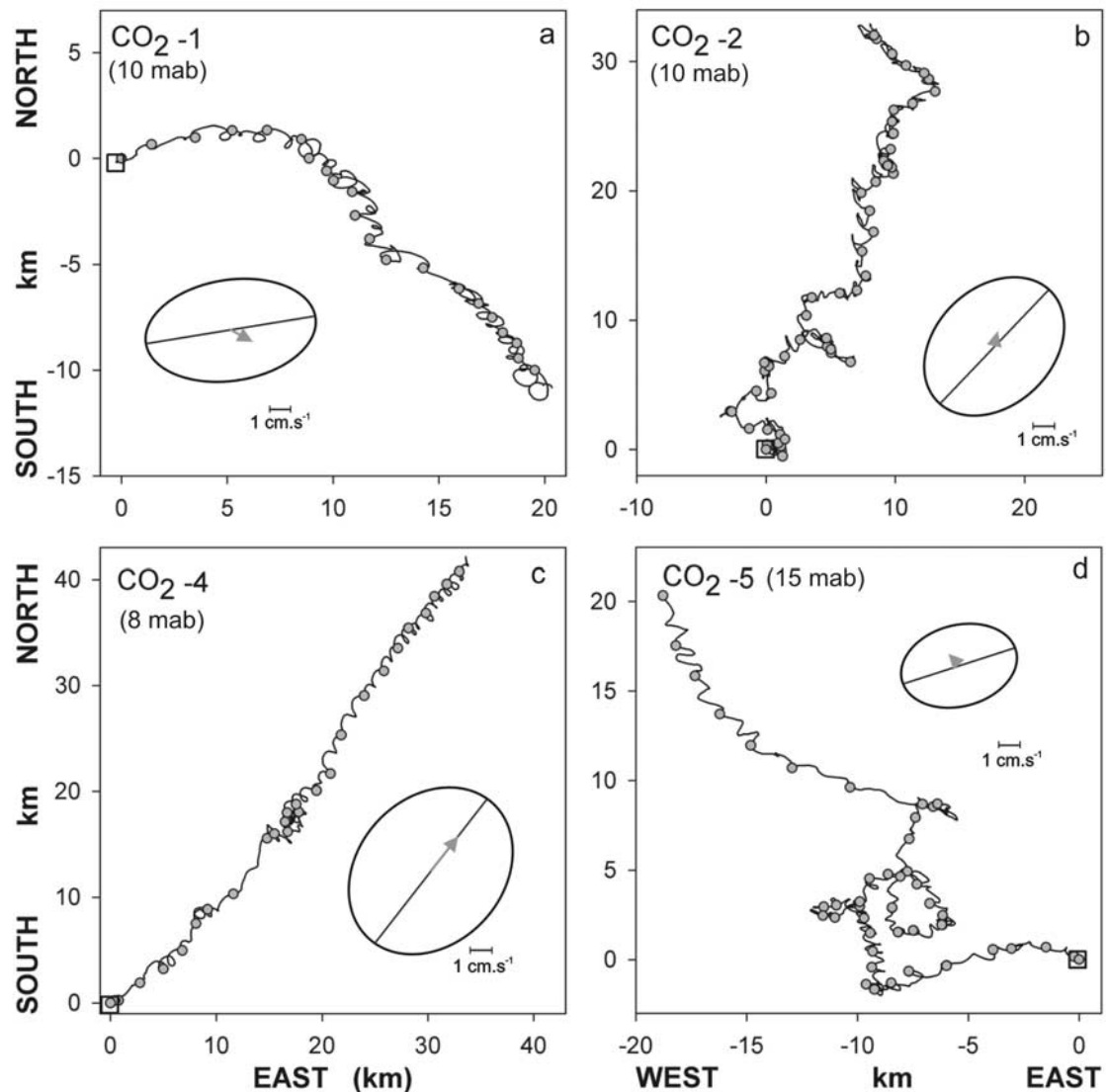


**Figure 5.** Progressive vectors plots for near-bottom currents measured during CO<sub>2</sub> release experiments. Small open box in each plot indicates starting location at beginning of experiment. A progressive vector indicating the directional flow sequence during each experiment is indicated by the black oscillating line. Start of each day marked by shaded circles. Principal axes of flow are indicated by an ellipse in each panel, in which major and minor axes represent one standard deviation of the mean current magnitude. Mean flow indicated by shaded arrow (same scale as principal axes ellipse). Height of the current measurements above the seafloor for each plot are indicated as meters above bottom (mab). (a) CO<sub>2</sub>-1. (b) CO<sub>2</sub>-2. (c) CO<sub>2</sub>-4. (d) CO<sub>2</sub>-5.

**Table 2.** Summary of Current Measurements and Estimates of Dissolution Rates for CO<sub>2</sub> Release Experiments<sup>a</sup>

Experiment	Interval, s	Data, hours	Magnitude Mean, cm s <sup>-1</sup>	Net Flow, cm s <sup>-1</sup>	Net Direction	$K_{\text{eddys}}$ cm <sup>2</sup> s <sup>-2</sup>	CO <sub>2</sub> Dissolution
CO <sub>2</sub> -1	598	1198	4.3	1.22	119.4	11.06	rapid
CO <sub>2</sub> -2	360	1166	4.4	0.81	29.3	11.81	rapid
CO <sub>2</sub> -3	n.d.	n.d.	n.d.	n.d.	n.d.	n.d.	slow
CO <sub>2</sub> -4	300	667	5.7	2.29	36.7	17.17	rapid
CO <sub>2</sub> -5	299	1016	2.9	0.77	312.2	5.36	slow

<sup>a</sup>Flow data calculated from a single acoustic Doppler current profiler 8 m above the seafloor for each experiment listed. No flow data were recovered for CO<sub>2</sub>-3. Interval indicates the sampling interval (s) during each experiment. Magnitude represents the mean nondirectional current speed. Net flow is average net transport toward net direction. Eddy kinetic energy is calculated from  $u'$ ,  $v'$ , and  $w'$ . Estimates of CO<sub>2</sub> dissolution rates are based on remotely operated vehicle observations of liquid CO<sub>2</sub> remaining in corals at the end of each experiment.

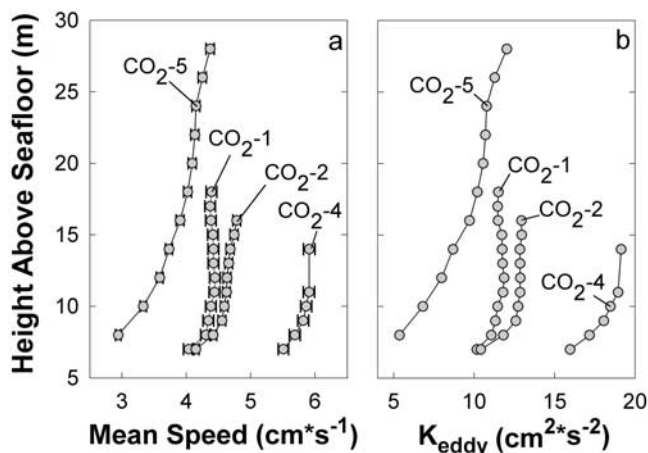


**Figure 6.** Mean current speed and eddy kinetic energy for CO<sub>2</sub> release experiments. (a) Vertical profiles of mean current nondirectional current speed (error bars represent 95% confidence limits) based on all available acoustic Doppler current profiler (ADCP) data from each experiment. (b) Vertical profiles of eddy kinetic energy, based on  $u'$ ,  $v'$ , and  $w'$ . Note the large difference in mean speed between CO<sub>2</sub>-5 and CO<sub>2</sub>-4 for both mean speed and eddy kinetic energy. Note also the decreased energy nearer the seafloor.

at sites A or B, and net drift was aligned tightly with the major principal axis of flow (Table 2, Figure 5c) in the along-canyon axis. Flow was consistently in the up-canyon direction, a pattern which has been observed elsewhere along the axis of Monterey Canyon (J. P. Barry et al., unpublished data, 2004). Mean current speed, net transport and eddy kinetic energy were each roughly 2–3 times greater than measured at the noncanyon sites. The apparent rate of CO<sub>2</sub> dissolution during this experiment was rapid, based on the observation of completely empty corrals at the end of the 31 day experiment.

[31] In contrast to the relatively energetic currents during CO<sub>2</sub>-4, flow at site A during CO<sub>2</sub>-5 was the most sluggish observed in any experiment, and was associated with very slow rates of CO<sub>2</sub> dissolution (Figure 6). The mean speed ( $2.9 \text{ cm s}^{-1}$ ) and net drift ( $0.8 \text{ cm s}^{-1}$ ) measured during CO<sub>2</sub>-5 were roughly half the speeds measured in Monterey Canyon during CO<sub>2</sub>-4. Eddy kinetic energy ( $5.4 \text{ cm}^2 \text{ s}^{-2}$ ), which probably plays the largest role in CO<sub>2</sub> dissolution from seafloor corrals, was only 31% of that observed during CO<sub>2</sub>-4.

[32] Flow patterns during CO<sub>2</sub>-1 and CO<sub>2</sub>-2 were intermediate in energy between the high energy flow during CO<sub>2</sub>-4 and very sluggish flow observed during CO<sub>2</sub>-5. Mean absolute current speeds and eddy kinetic energy for CO<sub>2</sub>-1 and CO<sub>2</sub>-2 were both near  $4.4 \text{ m s}^{-1}$  and  $2.3 \text{ cm}^2 \text{ s}^{-2}$ , respectively, though these were performed at two different sites. Even though net transport during CO<sub>2</sub>-1 ( $1.2 \text{ cm s}^{-1}$ ) was much higher than during CO<sub>2</sub>-1 ( $0.8 \text{ cm s}^{-1}$ ) the major and minor axes of flow were similar (ellipses in Figures 5a and 5d), leading to comparable levels of eddy turbulence near the seafloor. Site B is located along the base of the continental rise off central California, where flow during CO<sub>2</sub>-2 (Figure 5b) may have followed the general path of bottom contours

(Figure 1). No current data were recovered during CO<sub>2</sub>-3 due to instrument failure.

[33] Spectral analyses of current time series showed that periodic flow at all sites was dominated by the semidiurnal lunar constituent  $M_2$  (period  $\sim 12.4 \text{ h}$ ). The lunisolar diurnal ( $K_1 = 23.9 \text{ hours}$ ) and principal lunar diurnal ( $O_1 = 25.8 \text{ hours}$ ) constituents contained the greatest energy density for some components of flow. Spectra calculated from eastward flow for each experiment were nearly uniformly dominated by  $M_2$  (Figure 7, right column). Spectra generated using northward, absolute magnitude, or flow heading yielded generally similar results, with some variation in the importance of  $M_2$ ,  $K_1$ ,  $O_1$ , and other constituents. Spectra based on current magnitude (Figure 7, left column), matched most closely the spectral patterns of pH records (see below).

### 3.2. CO<sub>2</sub> Dissolution and pH Variability

[34] Rates of CO<sub>2</sub> dissolution varied among experiments, based on qualitative observations of differences in the amount of liquid CO<sub>2</sub> remaining in CO<sub>2</sub> corrals at the end of each experiment (Figure 2), and appear to be related to the magnitude of eddy kinetic energy measured during each experiment (Table 2). High rates of dissolution were observed during CO<sub>2</sub>-1, CO<sub>2</sub>-2, and CO<sub>2</sub>-4 (Figures 2c, 2d, and 2f). During CO<sub>2</sub>-1,  $\sim 20 \text{ L}$  of liquid CO<sub>2</sub> dissolved from each corral in only 2–3 weeks. In CO<sub>2</sub>-2 ( $\sim 100 \text{ L}$ ) and CO<sub>2</sub>-4 ( $\sim 20 \text{ L}$  per corral), near-complete dissolution of injected CO<sub>2</sub> was observed after 41 and 29 days, respectively. Because only a small amount of hydrate (CO<sub>2</sub>-2 (Figure 2d)) or no liquid CO<sub>2</sub> or hydrate (CO<sub>2</sub>-4) was remaining at the end of these experiments, the majority of dissolution may have occurred prior to the end of the experiments.

[35] Eddy kinetic energy was high during all three of these experiments (Table 2). Dissolution rates during CO<sub>2</sub>-3 were difficult to estimate, due to the refilling of the corral midway through the experiment, and the apparent formation of entrainment of water during CO<sub>2</sub> hydrate that appeared to have formed within the CO<sub>2</sub> pool. The corral was approximately 70% full at the end of the experiment (Figure 2e), reflecting either sluggish dissolution or significant hydrate formation (and seawater entrainment [Brewer et al., 1999]), or both. Unfortunately, no flow data were recovered during CO<sub>2</sub>-3. Dissolution during CO<sub>2</sub>-5 was slow. Several CO<sub>2</sub> corrals used in CO<sub>2</sub>-5 remained partially (1/8 to 1/2 full) of liquid CO<sub>2</sub> after 30 days, very likely related to the low mean current speeds and low turbulence measured at the site during this experiment.

[36] The magnitude and variability of pH perturbations varied among experiments, related to experimental design, distance from CO<sub>2</sub> pools (Figure 8), and current variability at each site. Shifts in pH caused by the CO<sub>2</sub> dissolution plume were highly variable and periodic during point source CO<sub>2</sub> experiments with centrally positioned CO<sub>2</sub> pools surrounded by study organisms and sensors (experiments CO<sub>2</sub>-1, -2, -3).

[37] The greatest pH changes were measured during experiment CO<sub>2</sub>-1, as reported by Barry et al. [2004]. Excursions of up to  $-1.7 \text{ pH}$  units were measured within 1 m of the CO<sub>2</sub> pools during this experiment, related to the very near proximity of pH sensors to experimental CO<sub>2</sub>



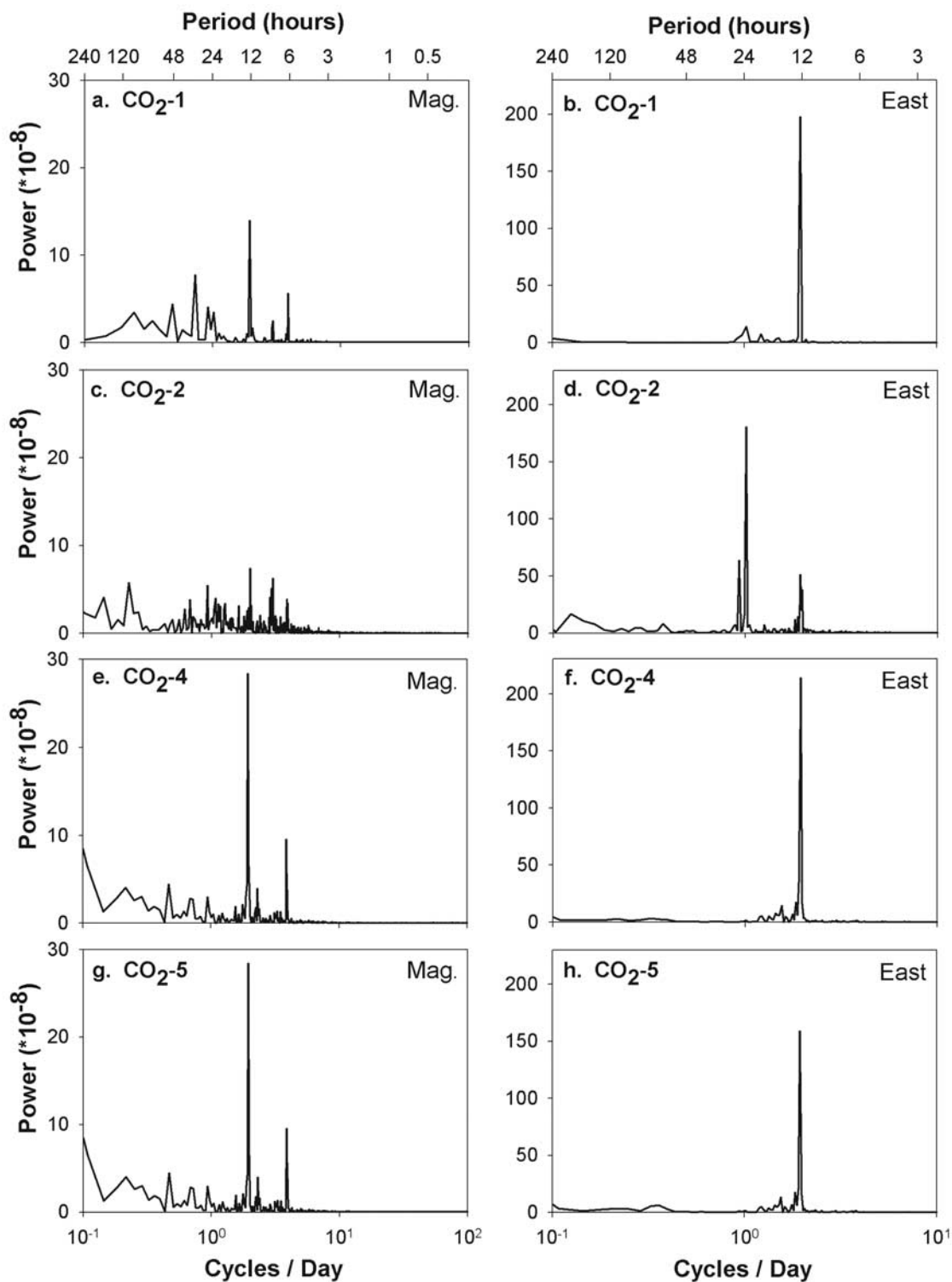


**Figure 7.** Spectral analyses of near-bottom currents during CO<sub>2</sub> release experiments. Left column includes spectra generated from time series of absolute current speed (Mag.). Right column displays spectra generated from time series of eastward current velocity (East). (a, b) CO<sub>2</sub>-1, site A. (c, d) CO<sub>2</sub>-2, site B. (e, f) CO<sub>2</sub>-4, site C. (g, h) CO<sub>2</sub>-5, site A. Note the strong periodicity at ~12.4 hours, representing the *M*<sub>2</sub> tide. Height above bottom for current measurements in each experiment is indicated in Figure 5.

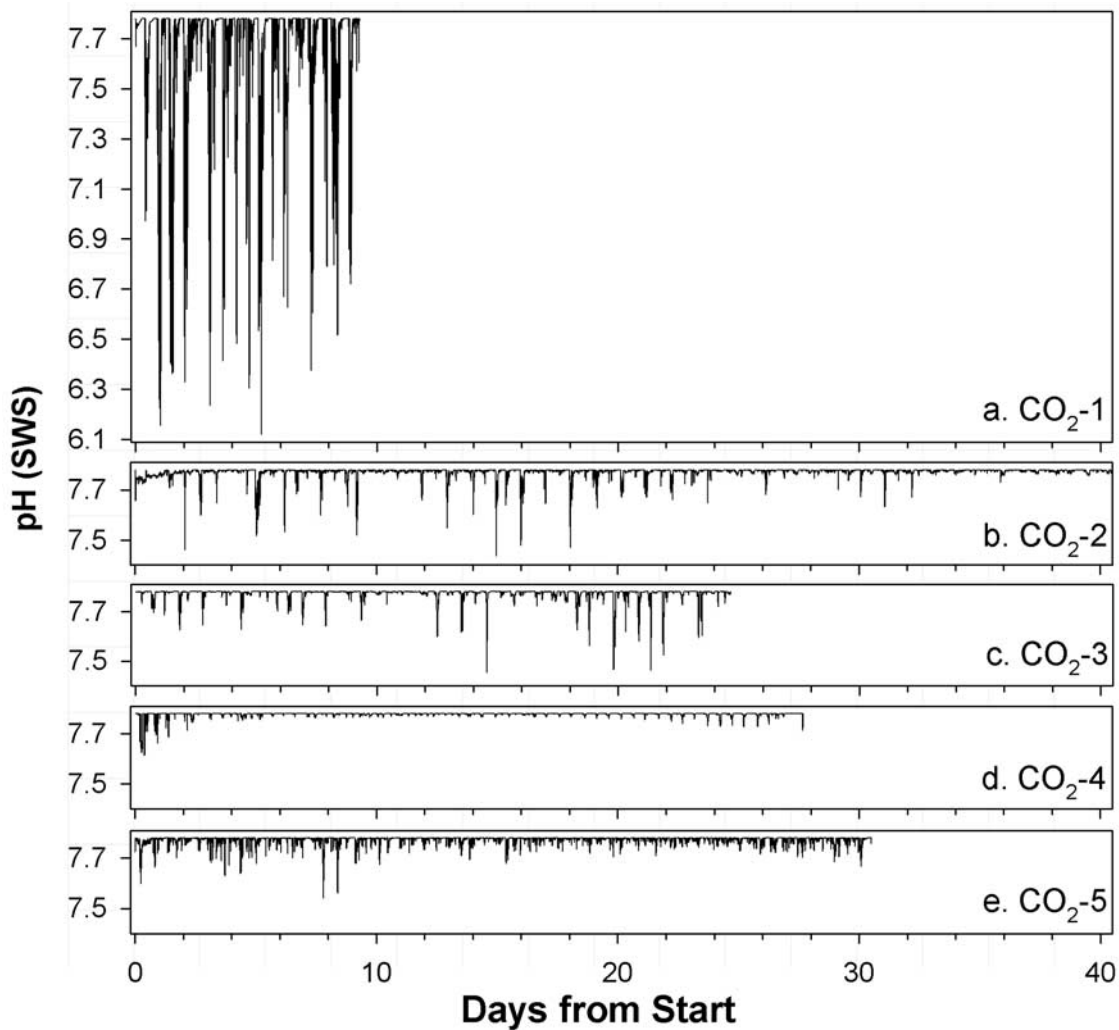


**Figure 8.** Time series of adjusted pH measurements during part of each CO<sub>2</sub> release experiment. (a) Release experiment CO<sub>2</sub>-1 (distance between pH sensor and CO<sub>2</sub> pool = 0.5 m), (b) CO<sub>2</sub>-2 (5 m), (c) CO<sub>2</sub>-3 (5 m), (d) CO<sub>2</sub>-4 (2.5 m), and (e) CO<sub>2</sub>-5 (5 m). Height of sensors above seafloor was ~3 cm. Note the strong diurnal periodicity in Figures 8a–8c and higher-frequency variation in Figures 8d and 8e. pH adjustments were applied to all data (see text). The magnitude of pH perturbations during CO<sub>2</sub>-4 are suspected to be erroneous. The length of all data records is near the total duration of each experiment, except for a (CO<sub>2</sub>-1), in which this pH sensor failed after 9 days during the 36 day experiment.

pools (Figure 8a). Perturbations in pH were highly periodic, however, indicating that the variable speed and direction of near-bottom currents controlled the advection of the dissolution plume and bathed the seafloor (i.e., pH sensor) alternately with the CO<sub>2</sub> dissolution plume and ambient seawater (pH = 7.78 SWS). Owing to the rotary character of near-bottom currents dominated by the *M*<sub>2</sub> tides, large reductions in pH occurred nearly every 12.4 hours, followed by periods of normocapnia (pH = 7.78). Extreme excursions in pH (>0.5 units) were rare, and the average pH during the experiment was 7.64 ( $\Delta$ pH = -0.14 units), with near-background values (7.78) through most of the experiment (Figure 9a). Unfortunately, only one of three pH sensors functioned reliably during the experiment, and this sensor also failed after ~10 days. In addition, though no pH data were collected near control corrals without CO<sub>2</sub>, subsequent experiments indicated that pH perturbations

near control corrals ~50 m away were nearly undetectable (i.e.,  $\Delta$ pH < 0.01 units).

[38] The central position of liquid CO<sub>2</sub> pools during experiments CO<sub>2</sub>-2 and CO<sub>2</sub>-3 produced a pattern of periodic pH variability similar to CO<sub>2</sub>-1. Unfortunately, pH sensors very near (~0.5 m) CO<sub>2</sub> pools failed in both experiments, preventing comparison of pH changes for that distance with those measured during CO<sub>2</sub>-1. Maximum pH excursions during CO<sub>2</sub>-2 and -3 (approximately -0.3 units) were much smaller than measured during CO<sub>2</sub>-1 (Figures 8b and 8c, Table 3), due to the greater distance (5 m) between sensors and CO<sub>2</sub> corrals and perhaps also to slightly lower rates of CO<sub>2</sub> dissolution. As in CO<sub>2</sub>-1, the exposure of organisms and sensors to the dissolution plume around CO<sub>2</sub> corrals was brief and episodic, with hypercapnic events approximately every 12 hours in association with the clockwise rotation of the *M*<sub>2</sub> tide. Seawater with near

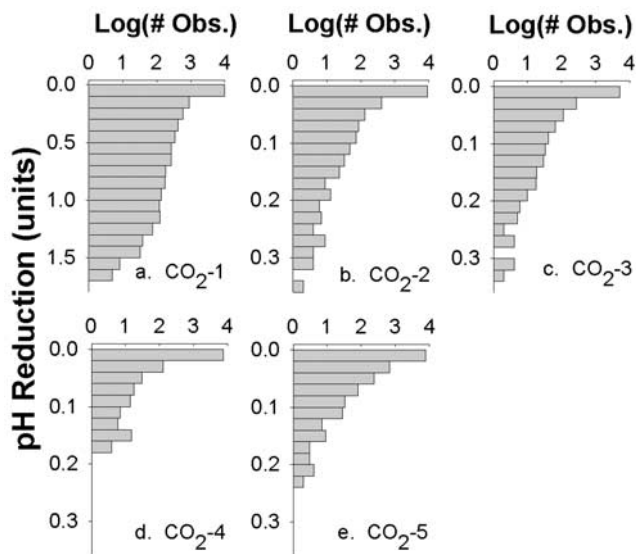


**Figure 9.** Frequencies of pH perturbations during CO<sub>2</sub> release experiments. Bars represent the number of observations during each experiment with shifts in pH of increasing magnitude (from a baseline of pH = 7.78 SWS). (a) CO<sub>2</sub>-1. (b) CO<sub>2</sub>-2. (c) CO<sub>2</sub>-3. (d) CO<sub>2</sub>-4. (e) CO<sub>2</sub>-5. Note the log scale of frequencies and the overwhelming dominance of very mild or no pH reduction for all experiments.

normal pH ( $\Delta\text{pH} < 0.05$  units) persisted more than 95% of the time, with excursions in  $\text{pH} > 0.1$  units accounting for only  $\sim 2\%$  of the pH measurements during these experiments (Figures 9b and 9c). The magnitude and temporal variability of pH reductions measured 5 m from CO<sub>2</sub> pools for CO<sub>2</sub>-2 and CO<sub>2</sub>-3 was quite similar for  $\sim 25$  days, just prior to the end of CO<sub>2</sub>-3. Because the corrals were not refilled during CO<sub>2</sub>-2, it appears that dissolution diminished, as indicated by the reduced pH variability (and lessened hypercapnic stress) during the latter half of this experiment (Figure 8b).

[39] Spectral analyses of pH time series (Figures 10a–10c) and current measurements (Figures 7a–7c) made during point source CO<sub>2</sub> release experiments CO<sub>2</sub>-1 to CO<sub>2</sub>-3 confirmed the importance of oscillatory, near-bottom currents in the advection and dispersal of the CO<sub>2</sub> dissolution plume, and the very similar pattern of pH variability among these experiments. In addition to the  $M_2$  tide, diurnal periodicity associated with the  $K_1$  tide was evident in both the flow and pH variation at site B during CO<sub>2</sub>-2. The  $M_4$  tide (6.2 hours) was secondary in importance at site A for pH and bottom currents.

[40] CO<sub>2</sub> enclosure experiments CO<sub>2</sub>-4 and CO<sub>2</sub>-5, in which organisms and sensors were encircled by three or seven CO<sub>2</sub> corrals, respectively, were expected to produce somewhat more stable shifts in pH, as desired for investigations of the sensitivities of deep sea organisms to hypercapnia. Performance of pH sensors was poor during CO<sub>2</sub>-4, and the adjustment required to remove drift was large, reducing our confidence in the magnitude, but perhaps not the periodicity, of pH changes in this experiment (Figure 8d). Exposure to the CO<sub>2</sub> dissolution plume from surrounding pools of liquid CO<sub>2</sub> was more frequent during these experiments due to the multiple CO<sub>2</sub> sources, but pH

shifts were generally mild ( $\Delta\text{pH} < 0.1$  units) and short lived (Figures 8d and 8e). Maximum pH reductions were near 0.2 units, and the average shift in pH during each experiment was only  $-0.008$  units (Table 3). This low average pH shift is due to the high percentage of mild pH perturbations; more than 99 and 97% of all observations during experiments CO<sub>2</sub>-4 and CO<sub>2</sub>-5, respectively, showed pH changes of  $-0.05$  units or less (Figures 8d and 8e).

[41] Even though the shifts in pH were small, experimental plots (i.e., animals, sensors) were exposed more frequently to the CO<sub>2</sub> plume during each of the CO<sub>2</sub> enclosure experiments than during point source CO<sub>2</sub> release experiments. The variance:mean ratio for pH measurement during CO<sub>2</sub> enclosure experiments (Table 3) was low, indicating a more stable pH field than was found for point source experiments. The greater frequency of hypercapnic events during CO<sub>2</sub> enclosure experiments is evident in Figures 8d and 8e, showing the time series of pH perturbations, and Figures 11d and 11e, characterizing pH variability in the lower 1 m of the water column during 10 days of each experiment. The less frequent and staccato character of pH events during earlier point source experiments is driven by the dominance of the  $M_2$  barotropic tide on bottom currents. During CO<sub>2</sub> enclosure experiments, the frequent, though milder, perturbations indicate a partial decoupling of the pH field from the periodicity of bottom currents.

[42] Spectral analyses also indicated the higher frequency of hypercapnic events. Although the  $M_2$  tide exerted strong dominance over pH variability within the triangular enclosure of CO<sub>2</sub> corrals during CO<sub>2</sub>-4, variability was also observed on shorter frequencies not observed in near-bottom currents at the site (Figures 7e, 7f, 9d, and 10d). The persistent up-canyon flow within Monterey Canyon at site C may also have reduced both the residence time and recirculation of the dissolution plume within the experimental site. High-frequency variation in pH due to multiple CO<sub>2</sub> sources was most evident during CO<sub>2</sub>-5. Spectral density is mixed among several nontidal frequencies in the center of the enclosure (Figure 9e), with the greatest energy at a period of 4.6 hours.

### 3.3. Biological Responses of Benthic Meiofauna to Hypercapnia

[43] The effects of exposure to the acute hypercapnia very near CO<sub>2</sub> corrals during the first CO<sub>2</sub> release experiment

**Table 3.** Summary of pH Perturbations During CO<sub>2</sub> Release Experiments<sup>a</sup>

	CO <sub>2</sub> -1	CO <sub>2</sub> -2	CO <sub>2</sub> -3	CO <sub>2</sub> -4	CO <sub>2</sub> -5
Max	7.78	7.78	7.78	7.78	7.78
Min	6.12	7.44	7.45	7.61	7.54
Mean	7.64	7.77	7.77	7.78	7.77
SD	0.28	0.02	0.03	0.01	0.02
N	13,363	10,018	5921	7977	8790
	<i>Deviations</i>				
Max	-1.660	-0.342	-0.326	-0.166	-0.239
Mean	-0.142	-0.008	-0.008	-0.003	-0.008
SD	0.275	0.023	0.025	0.011	0.017
S <sup>2</sup> : mean	0.533	0.066	0.078	0.040	0.036

<sup>a</sup>Deviations for pH measurements are shown in lower rows. The pattern of maximum perturbations is related principally to distance from CO<sub>2</sub> pools, rather than its design.

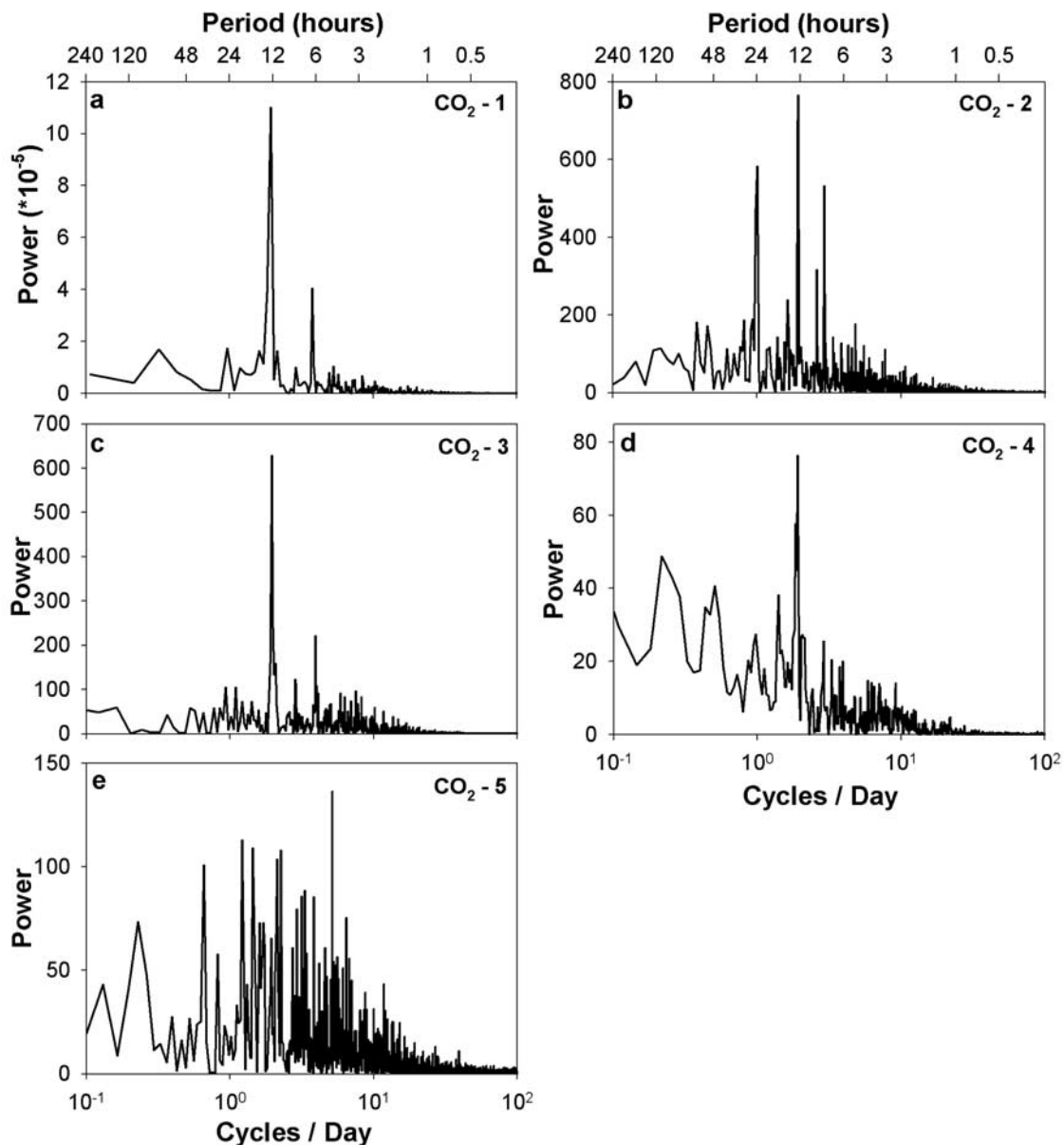


**Figure 10.** Power spectra for pH variability during CO<sub>2</sub> release experiments. (a) CO<sub>2</sub>-1. (b) CO<sub>2</sub>-2. (c) CO<sub>2</sub>-3. (d) CO<sub>2</sub>-4. (e) CO<sub>2</sub>-5. Note differences in y axis scale among figures and the strong periodicity near 12.4 hours ( $M_2$  tidal flow) for point source CO<sub>2</sub> experiments (Figures 10a–10c) and weaker, higher-frequency periodicity for CO<sub>2</sub> enclosure experiments (Figures 10d and 10e).

(CO<sub>2</sub>-1) were severe, as reported by Barry *et al.* [2004]. All major meiofaunal taxa (nematodes, flagellates, amoebae) experienced high (>90%) mortality within 0.5 m of CO<sub>2</sub> pools after 30 days of exposure to episodic reductions in pH of up to  $-1.6$  pH units. In contrast, mortality near control corals was minor or undetectable.

[44] The effects of hypercapnia and acidosis on benthic meiofauna varied among regression design CO<sub>2</sub> release experiments (CO<sub>2</sub>-2 and CO<sub>2</sub>-3) that we examine in this paper. Although the pattern and intensity of pH variability was similar for these two experiments (Table 3), changes in meiofaunal abundance (i.e., survival rates) differed. Unlike the severe hypercapnia and high meiofaunal mortality observed during experiment CO<sub>2</sub>-1, the abundance of nematodes, flagellates, and amoebae did not change with

distance from the central CO<sub>2</sub> pools during experiment CO<sub>2</sub>-2 after 41 days of episodic, moderate hypercapnia. During CO<sub>2</sub>-3, nematodes did not vary in abundance with distance from the CO<sub>2</sub> pool, but flagellates and amoebae each decreased significantly ( $p < 0.005$ ) closer to CO<sub>2</sub> pools by the end of the experiment. Survival nearest the CO<sub>2</sub> pool was only  $\sim 30\%$ , but increased to 75% survival 10 m from the pool (Figures 12d and 12e).

## 4. Discussion

### 4.1. Efficacy of pH Perturbations During CO<sub>2</sub> Release Experiments

[45] A highly stable shift in seawater chemistry desirable for studies of tolerance to hypercapnia was not observed

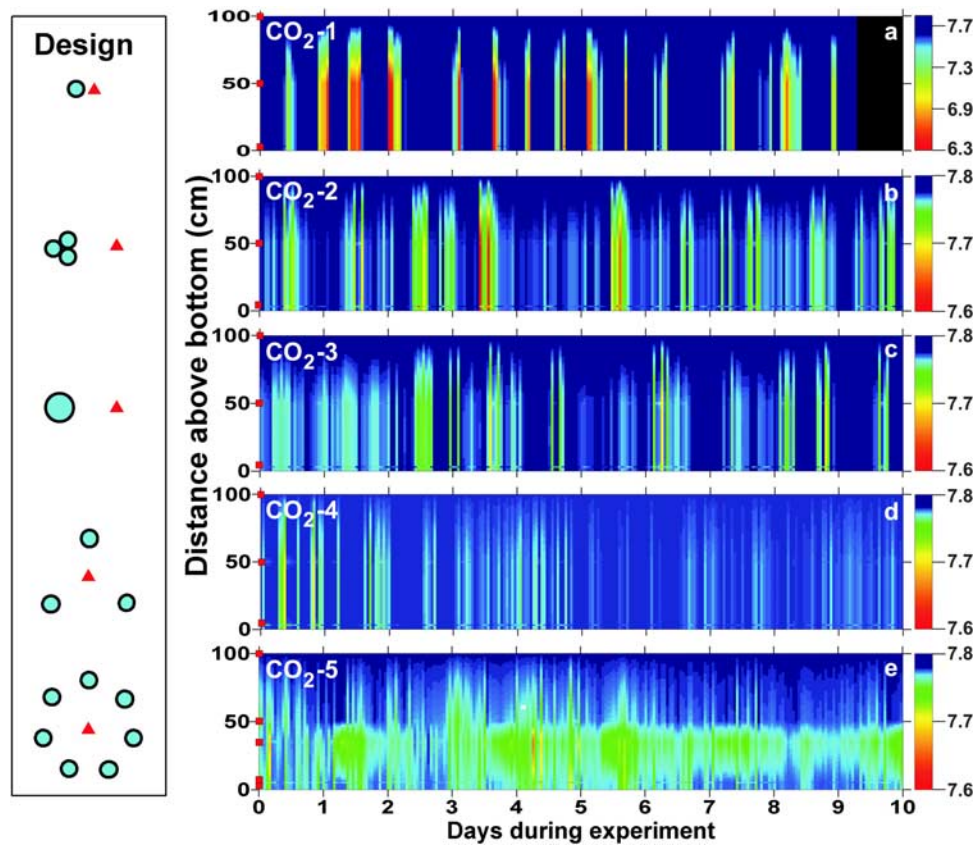


**Figure 11.** Time series of seawater pH to 1 m above the seafloor during CO<sub>2</sub> release experiments. (left) Layout of CO<sub>2</sub> pools (blue circles) and pH sensors (red triangles) during each experiment. (right) pH changes during 10 days of each CO<sub>2</sub> release experiment. Note scale difference between Figure 11a and Figures 11b–11e. Positions of pH sensors (red squares on left y axis) were  $\sim 3$  cm above bottom for CO<sub>2</sub> release experiments 1–4 (Figures 11a–11d), for which pH at 50 cm above bottom was not measured (assumed to equal the pH at 5 cm). For CO<sub>2</sub> enclosure experiment CO<sub>2</sub>-5 (Figure 11e), four pH sensors were located at 5 cm height, one at 35 cm, and one at 50 cm. Background pH (100 cm above seafloor) for all panels was assumed to be 7.78 (SWS). Note the roughly semidiurnal periodicity of pH perturbations for point source CO<sub>2</sub> release experiments with a central CO<sub>2</sub> pool (Figures 11a–11c) and high-frequency or more constant pH variability for CO<sub>2</sub> enclosure experiments (Figures 11d and 11e).

during any of the CO<sub>2</sub> release experiments. Instead, CO<sub>2</sub> concentrations (measured as pH) varied throughout all experiments, with the vast majority of observations near normal seawater pH. This high variability in CO<sub>2</sub> and pH stress impairs our ability to interpret the dose tolerance responses of animals to hypercapnia. It is not possible to partition the importance of episodic moderate hypercapnia or chronic mild hypercapnia during these experiments on animal survival. More useful experiments would provide relatively stable CO<sub>2</sub> perturbations within the range of variation expected in the future for surface or deep ocean [Hoffert *et al.*, 1979]. Enclosure designs used in this study, though not ideal, damped the high pH variation observed in point source experiments. Further studies to compare the impacts of episodic, severe hypercapnia with those arising from stable, but mild hypercapnia would improve our understanding of the dose tolerance patterns of deep sea animals. Information generated from such studies will serve as important inputs for models of ecosystem dynamics under various scenarios of future ocean chemistry.

[46] The interpretation of faunal responses to hypercapnia and acidosis was also complicated by the frequent failure, poor reliability, and considerable drift of pH sensors during these long-term, deep sea studies. The adjustment of raw pH data to fit both the expected background pH (7.78 SWS) and to remove the sometimes significant drift of each sensor may have eliminated some significant, though relatively small, pH perturbations. This pH adjustment method retains the larger spikes in pH variation very effectively, but sometimes removed small-scale variation in pH which might have represented real hypercapnic events. Development of more sophisticated sensors, including pH and CO<sub>2</sub> sensors for deep sea studies [Someya *et al.*, 2004], would catalyze progress in this area.

[47] Because we could not measure pore fluid pH throughout these experiments, we assumed that pH perturbations measured in the benthic boundary layer immediately above the seafloor would be correlated, or at least coupled, with pore fluid pH. Shipboard measurements of pore fluid pH reported by Thistle *et al.* [2005] for the upper sediment

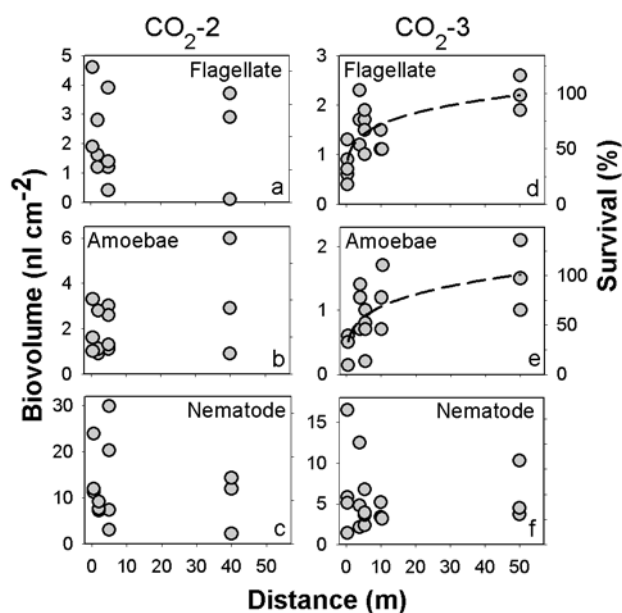


**Figure 12.** Variation in meiofaunal abundance at the end of CO<sub>2</sub> release experiments CO<sub>2</sub>-2 and CO<sub>2</sub>-3. (a, b, c) Results from CO<sub>2</sub>-2, sampled 48 days after CO<sub>2</sub> release. (d, e, f) Results from CO<sub>2</sub>-3, sampled 27 days after CO<sub>2</sub> release. Meiofaunal taxa are indicated in each panel. Abundance is measured as biovolume. Distance indicates distance from central CO<sub>2</sub> pools. Shaded dots indicate biovolume values for individual cores collected at the end of each experiment. Dashed black curves indicate statistically significant power functions ( $y = ax^b$ ) for flagellates ( $r^2 = 0.56$ ,  $p < 0.0004$ ) and amoebae ( $r^2 = 0.47$ ,  $p < 0.0017$ ) in CO<sub>2</sub>-3. Right axis indicates estimated survival, assuming that background biovolume values (i.e., 50 m from pool) represent zero CO<sub>2</sub>-related mortality.

layer (top 8 mm) near the center of the triangular CO<sub>2</sub> enclosure during CO<sub>2</sub>-4 showed pH reductions of  $\sim 0.6$  pH units compared to control areas. Measurements with in situ sensors we deployed just above the seafloor indicated much milder pH perturbations, however the accuracy of these sensors were suspect during this experiment. Therefore although the scaling of interstitial pH with the pH of the overlying water remains unclear, it is certain that the two are coupled. Additional study is required to resolve this relationship.

[48] Rates of dissolution for liquid CO<sub>2</sub> and CO<sub>2</sub> hydrate are poorly constrained, and are affected by the presence of CO<sub>2</sub> hydrate and the flow speed or strength of turbulence eddies near the CO<sub>2</sub>-seawater interface [Fer and Haugan, 2003; Rehder et al., 2004; Teng and Yamasaki, 2000]. Slow rates of CO<sub>2</sub> dissolution estimated for experiments CO<sub>2</sub>-3 and CO<sub>2</sub>-5 were likely related to low turbulence during these experiments, but may have been influenced by several other factors, including mean currents, sedimentation on the liquid CO<sub>2</sub>, formation of CO<sub>2</sub> hydrate, and the hydrodynamics of the CO<sub>2</sub> corral. The high aspect ratios (48 cm diameter  $\times$  40 cm high) and multiple corrals used during CO<sub>2</sub>-2 (Figures 2c and 2d) may have enhanced turbulence over the corrals, thereby accelerating dissolution. In con-

trast, the larger (91 cm diameter  $\times$  30 cm high) CO<sub>2</sub> pool used in CO<sub>2</sub>-3 may have impeded dissolution, particularly when partially full. Although the CO<sub>2</sub> surface in this large corral was near the top of the corral at the end of the experiment, seawater entrainment during hydrate formation [Brewer et al., 1999] may have increased the volume of the liquid-hydrate pool. Nevertheless, CO<sub>2</sub> dissolution appears to have been slow for such a large volume to remain after 1 month, perhaps due to sluggish currents, and the insulating effects of a veneer of sediment that was deposited on the hydrate surface of the pool during the experiment (likely caused by the ROV).

[49] The effects of CO<sub>2</sub> dissolution and hydration on seawater salinity [Brewer et al., 2005] suggest that salinity could be a useful proxy for pCO<sub>2</sub> or pH. Brewer et al. [2005] have shown that salinity initially drops during CO<sub>2</sub> dissolution, as liquid dilutes seawater, but finally rises to values greater than ambient values as CO<sub>2</sub> hydration reactions proceed to completion. Salinity varied considerably in each experiment, but its relationship to CO<sub>2</sub> chemistry could not be determined. CO<sub>2</sub> hydration proceeds considerably faster at depth than in surface waters, but there is insufficient time for hydration to equilibrate during the transit of the dissolution plume through our experimental plots. Because the system is in disequilibrium, the salinity data provide a complex view of CO<sub>2</sub> changes in the experiments. For this reason, we relied only on pH perturbations to estimate changes in CO<sub>2</sub> chemistry. Temperature variation was low ( $<0.2^\circ$ ) throughout each experiment and was not useful in estimating pH or CO<sub>2</sub> levels.

[50] Dominance of semidiurnal periodicity in pH during the point source CO<sub>2</sub> release experiments was not surprising, especially considering the magnitude of  $M_2$  tides along central California (Figure 7) [Beaulieu and Baldwin, 1998; Breaker and Broenkow, 1994; Filloux, 1971]. Baroclinic  $M_2$  tides, generated along the continental shelf break in Monterey Bay [Rosenfeld, 1990], may reflect seaward, increasing turbulence in offshore waters [Lien and Gregg, 2001], and could have contributed to the flow field measured in these experiments. Variation in the direction and speed of currents between experiments are likely caused by changes in the relative importance of factors contributing to abyssal current, including seasonal and interannual variability. Beaulieu and Baldwin [1998] noted large shifts in abyssal currents at station M in 4100 m depth off central California, attributing them to the “spring transition” characteristic of the west coast of North America. This seasonal shift caused by changes in the wind field at the surface has also been documented in the eastern North Atlantic [Dickson et al., 1982], and may have affected flow at site A.

[51] The tight coupling between current variability in the benthic boundary layer and the periodicity in pH perturbations during each experiment suggests that boundary layer flows measured 5 or more m above the seafloor extend to very near the seabed. Our flow measurements were no closer than 5–6 m above the seabed, which is above the log-layer (the range of depths where current speeds decreases scales according to the log of distance above the seabed, due to the frictional effects of the bottom). The log-layer for the flows observed in this study is expected to be  $\sim 2$ –3 m at deep sea depths [Gross et al., 1986].

*Beaulieu and Baldwin* [1998] estimated the boundary layer flow to the seabed from measurements of currents 2.5–600 m above the bottom at station M. Estimates of  $z_0$  (flow at the seabed) for station M ranged from 0.11 to 0.91 cm s<sup>-1</sup>, based on mean currents 2.5 m above the bottom of  $\sim 2\text{--}4$  cm s<sup>-1</sup>. Considering the similar mean flow speeds and bottom characteristics of station M to our study sites, flow at the seabed is likely to fall within the range estimated by *Beaulieu and Baldwin* [1998], and should vary roughly in proportion to the mean speed measured further above the bottom. Extrapolating the pattern of flow measured in the benthic boundary layer to the seabed during our experiments could explain the observed variation in apparent rates of CO<sub>2</sub> dissolution among experiments.

[52] The extent of pH variation in the triangular and circular CO<sub>2</sub> enclosure experiments was unexpected, however, even though the observed pH periodicity was generally higher in frequency than for point source CO<sub>2</sub> designs. The enclosure designs were expected to produce a more stable and more persistent pH perturbation within the enclosure, due to both the multiple CO<sub>2</sub> dissolution sources and some anticipated overlap in the dissolution plumes emanating from each pool. Although episodes of reasonably large pH perturbations (approximately  $-0.2$  pH units) were observed in all experiments, they were generally short lived in all but CO<sub>2</sub>-1, in which pH sensors were positioned very near the CO<sub>2</sub> pools. Terrestrial FACE CO<sub>2</sub> perturbation systems can also suffer from high pCO<sub>2</sub> variation (data available from <http://cdiac.esd.ornl.gov/programs/FACE/face.html>), but the active control of CO<sub>2</sub> injection for these systems provides much tighter control on mean and maximum changes in pCO<sub>2</sub> within enclosures.

#### 4.2. Biological Sensitivity of Benthic Meiofauna

[53] Mortality associated with hypercapnia was detected in most CO<sub>2</sub> release experiments, even though perturbations in pH were generally short lived, and in some cases, mild. High rates of mortality observed after even short-term exposure to pH reductions  $>1$  pH unit, as occurred during CO<sub>2</sub>-1 [*Barry et al.*, 2004] are not surprising, since such large changes in pH exceed greatly the range of natural environmental variability. Variation in the pH of the aerobic surficial layer of deep sea sediments is generally much less than one unit, and most meiofaunal taxa studied here may not experience this entire range [*Giere*, 1993]. During CO<sub>2</sub>-1, the close proximity of sediment samples to the CO<sub>2</sub> pools probably led to very high CO<sub>2</sub> perturbations in the upper sediment layer. Although we did not measure pH in sediments during CO<sub>2</sub>-1, cores collected from within CO<sub>2</sub> corrals which had been covered with liquid CO<sub>2</sub> effervesced to a depth of nearly 10 cm down-core upon recovery to the surface. This indicates a deep penetration of liquid CO<sub>2</sub> within the sediment (e.g., Figure 2b). Even though we did not observe similar CO<sub>2</sub> outgassing in sediment cores analyzed for meiofauna, the surface sediments surrounding the CO<sub>2</sub> corrals were likely quite hypercapnic.

[54] Perturbations of pH measured in CO<sub>2</sub>-2 and CO<sub>2</sub>-3 were relatively mild, ( $-0.1$  to  $-0.2$  pH units) and infrequent ( $<2\%$  of observations), but still led to upward of 30% mortality 5 m from CO<sub>2</sub> pools for flagellates and amoebae during CO<sub>2</sub>-3 (Figures 12d and 12e). This mortality rate suggests that pH perturbations were either more severe in

the sediment column than measured in the overlying water, or that these meiofaunal taxa are quite sensitive to relatively small and brief changes in pH. The contrasting results for the survival of flagellates and amoebae between CO<sub>2</sub>-2 and CO<sub>2</sub>-3 may be related to the longer duration of CO<sub>2</sub>-2, its smaller CO<sub>2</sub> dose, and apparently diminished dissolution toward the end of the experiment. Approximately 100 L of liquid CO<sub>2</sub> were released in the central pools used for CO<sub>2</sub>-2, for an experiment lasting 41 days. In contrast,  $\sim 150$  L were injected into the CO<sub>2</sub> corral used for CO<sub>2</sub>-3, (80 L after 17 days) during this much shorter experiment. Although much CO<sub>2</sub> remained at the end of CO<sub>2</sub>-3, its pH record (Figure 8c) suggests that hypercapnic stress was as high as or higher than during CO<sub>2</sub>-2. It is possible that meiofaunal survival was high during CO<sub>2</sub>-2, as suggested by the abundance patterns detected at the end of the experiment, or that the local population had recovered to some extent, by either immigration and/or population turnover as hypercapnic stressed lessened after the first month. Deep sea ciliate and flagellate generation times are not well known, but probably range near days to weeks, considering the growth rates of several hours for shallow planktonic ciliates [*Hansen and Bjornsen*, 1997]. The sensitivities of benthic meiofauna to CO<sub>2</sub> elevation during the triangular CO<sub>2</sub> enclosure experiment (CO<sub>2</sub>-4) were measured by *Carman et al.* [2004] and *Thistle et al.* [2005], who detected mortalities among meiofaunal harpacticoid copepods near 50% at the center of the triangular CO<sub>2</sub> enclosure. Although the abundances of harpacticoids and other meiofauna (nematodes, nauplii, kinorhynchs, polychaetes) were similar among control and hypercapnic samples, closer inspection of individuals from each indicated that  $\sim 50\%$  of animals in hypercapnic samples were partially degraded, indicated death prior to collection by the ROV. Profiles of pH within the sediment column within the enclosure compared to those from a control site  $\sim 50$  away indicated a pH reduction of nearly 0.6 pH units in the upper sediment column.

[55] Patterns of mortality for benthic meiofauna detected during these experiments are somewhat mixed, but in most experiments (all but CO<sub>2</sub>-2) suggests that chronic acidosis and hypercapnia that may be typical in the future ocean could have large effects on benthic meiofaunal populations. Maximum perturbations in pH at a distance of  $\sim 5$  m was generally in the range of  $-0.2$  pH units in the overlying water, or perhaps greater in the pore fluid [*Thistle et al.*, 2005], but these hypercapnic events were short lived, and rare (pH was most often very near normocapnic). Even after exposure to infrequent, relatively mild hypercapnia in the overlying bottom water, meiofaunal mortality in two of three experiments (CO<sub>2</sub>-3, -4) was near 30% or more. The impacts of chronic hypercapnia are expected to be more severe.

[56] The large variation in pH observed in the CO<sub>2</sub> release experiments limits our ability to determine key thresholds of hypercapnia that could trigger physiological stress or death for any of the animals studied. An understanding of the biological and ecological consequences of increased hypercapnia over shallow and deep waters of the world ocean will require knowledge of the physiological responses of organisms as a function of the severity and duration of hypercapnia. Thus thresholds (e.g., dose tolerance data) for individual survival, as well as information on

the effects of sublethal, but potentially energetically costly hypercapnic exposure, are most easily considered in terms of chronic, stable changes in pH by known intervals [Auerbach *et al.*, 1996]. A broad base of information concerning the dose tolerance responses of a phylogenetically and environmentally diverse set of animals, as well as the development of effective ecosystem models [deYoung *et al.*, 2004] may be important precursors to predicting ecosystem changes that may result from “business as usual” [Leggett *et al.*, 1992] changes in ocean chemistry.

[57] Exposure to hypercapnic, acidic seawater, from either direct CO<sub>2</sub> injection or the long-term increase in deep sea CO<sub>2</sub> levels drawn from atmospheric CO<sub>2</sub> emissions pose physiological challenges for marine animals that have a scope of tolerance to such stresses defined by their evolutionary history of adaptation to environmental variability. Optimal metabolic performance for most animals requires tight control (or narrow uncontrolled variability) of internal pH, which influences a variety of cellular physiological functions [Hochachka and Somero, 2002]. Owing to the reduced environmental variability typical of deep sea environments [Kennett and Ingram, 1995], coupled with apparently strong selection for adaptations to minimize energy requirements in deep, typically food-poor ocean environments, deep sea animals often exhibit higher sensitivities to environmental variation than their shallow-water counterparts (or hydrothermal vent taxa), including variation in pH and CO<sub>2</sub> [Seibel and Walsh, 2003]. Thus while animals that typically experience large pH variation may have the physiological capacity to maintain internal acid/base balance even during severe hypercapnic events (e.g., hydrothermal vents animals [Goffredi *et al.*, 1998]), most deep sea animals may not survive even milder hypercapnia.

[58] Meiofauna, including those studied here, are expected to be equipped poorly to tolerate acidosis. Flagellates, amoebae, and nematodes are primitive groups that rely on diffusion through cell membranes for respiration. The absence of respiratory proteins in these groups may limit the potential impacts of hypercapnia on oxygen binding that can be acute in some more complex taxa [Seibel and Walsh, 2003], and tolerance to hypercapnia may be restricted by the inability of most taxa to maintain acid-base balance within normal levels. Diffusion of CO<sub>2</sub> through cell membranes will quickly equilibrate the CO<sub>2</sub> tensions and pH of intra and extracellular fluids with ambient seawater concentrations. Nematodes, with their thicker cuticle, may be buffered somewhat more effectively than flagellates and amoebae from brief pH events, but persistent changes in seawater chemistry will swamp the internal fluids of all of these taxa rather quickly. At present, the key cellular processes impacted by hypercapnia or acidosis for these taxa remain unknown.

### 4.3. Future Studies of the Impacts of Hypercapnia on Deep Sea Ecosystems

[59] In view of the nearly inevitable continuing rise in atmospheric CO<sub>2</sub>, the world ocean is faced with a hypercapnic future that may rival levels unseen for upward of 100 million years, with potentially large changes in the ecosystem patterns and function of the oceans. Progress in understanding the consequences of elevated CO<sub>2</sub> levels

on marine populations and communities depends on our ability to measure the response of organisms to changes in CO<sub>2</sub>, pH and perhaps other factors. Although laboratory studies of physiological performance are possible for shallow water species, in situ studies are required for most deep sea species [Shirayama, 1998], at least for water depths exceeding ~1500 m, owing to their general intolerance of surface pressures. Capture of animals at depth, and return to the laboratory under in situ pressure and temperature is possible, and should supplement field studies. In many cases, however, field experiments that provide tight control over seawater chemistry can be used to measure at least the short-term response of various species to perturbations in CO<sub>2</sub> and pH. Our experimental approach provides some inference concerning the sensitivity of some deep sea species to hypercapnia, but do not determine the range of pH and CO<sub>2</sub> perturbations tolerable for survival (e.g., LD<sub>50</sub>). Nor have deep sea experiments to date measured the sublethal consequences of hypercapnia that may have important negative consequences for populations. For example, Kurihara *et al.* [2004] used laboratory experiments to demonstrate that littoral sea urchins and copepods exposed to moderate hypercapnia experienced reduced rates of growth, developmental delays, and anomalies (sea urchins) and reduced reproductive success (fertilization: urchins, egg production and hatching: copepods). Likewise, Auerbach *et al.* [1996] and Caulfield *et al.* [1997] compiled data on the dose tolerance (survival rates) of a variety of shallow water marine organisms, providing the first overview of the general pattern of pH (and hypercapnia) stress tolerance of marine organisms. Shirayama [1998, p. 381] noted that deep sea species have “1) Low biological activities, 2) Long life span, 3) High sensitivity to the environmental disturbance, 4) High species diversity, and 5) Low density,” suggesting that they are hypersensitive to environmental disturbance. Seibel and Walsh [2001] examined metabolic performance data for a variety of species inhabiting depths from 0 to ~1500 m, suggesting that deep water species are potentially orders of magnitude more sensitive to CO<sub>2</sub>-related stresses than their shallow water counterparts. The role of the intense eastern Pacific oxygen minimum, which is confounded with depth in their data set, remains to be examined.

[60] Future in situ studies will require more sophisticated designs and perhaps significantly more complex subsea instrumentation to provide stable perturbations in CO<sub>2</sub> and pH levels that will allow researchers to examine the dose tolerance responses of deep sea taxa to changes in seawater chemistry caused by ocean carbon sequestration or long-term increases in CO<sub>2</sub>. Several alternatives are possible, from in situ collections of deep sea organisms returned to surface laboratories under pressure for controlled physiological study, to deep sea mesocosms akin to those developed for CO<sub>2</sub> studies in terrestrial systems, or automated in situ chamber systems capable of small-scale metabolic studies. FACE experiments [McLeod and Long, 1999] are underway at dozens of sites across the globe to measure the response of terrestrial communities to elevated CO<sub>2</sub> levels. FACE studies regulate pCO<sub>2</sub> over replicated terrestrial plots, based on rapid air flow sensors and sophisticated upstream CO<sub>2</sub> injectors. Similar efforts, representing an advanced form of our CO<sub>2</sub> enclosure designs may be required for



ocean studies before either the determination of dose responses, or the effects of chronic, long-term hypercapnia on most marine species can be examined.

[61] While the application of FACE technology may be productive in understanding the impacts of increasing CO<sub>2</sub> levels in the oceans, the spatial and temporal scales, and focus on specific habitats relevant for ocean studies must be considered. Deep sea bathypelagic and sediment habitats, which dominate ocean ecosystems, may require vastly different applications of mesocosm-like technology. Unlike terrestrial systems, marine microbial processes often dominate carbon cycling in deep sea ecosystems. Thus the appropriate spatial scale of experimental enclosures may be quite small. Pelagic habitats also present complex technical challenges for controlled volume experiments. Automated small-scale in situ chamber systems capable of measuring metabolic responses of individual animals or sediment samples to hypercapnia may represent the most productive technological developments for studies of the biology of a high-CO<sub>2</sub> ocean.

[62] **Acknowledgments.** These studies were supported by the Monterey Bay Aquarium Research Institute (project 200002), the Ocean Carbon Sequestration Research Program, Biological and Environmental Research (BER), U.S. Department of Energy (awards DE-FG03-01DF63065 and DE-FG02-04ER63721), and the National Energy Technology Laboratory (NETL), U.S. Department of Energy (award DE-FC26-00NT40929). We are particularly grateful to P. Brewer, E. Peltzer, and P. Walz for their assistance in the field studies and to the outstanding support from the crews of the R/V *Western Flyer* and the ROV *Tiburon*. Two anonymous referees provided valuable comments concerning the format and content of the manuscript.

## References

- Allen, L. H., Jr. (1992a), Field techniques for exposure of plants and ecosystems to elevated CO<sub>2</sub> and other trace gases, *Crit. Rev. Plant Sci.*, *11*, 85–119.
- Allen, L. H., Jr. (1992b), Free-Air CO<sub>2</sub> Enrichment field experiments: An historical overview, *Crit. Rev. Plant Sci.*, *11*, 121–134.
- Allen, L. H., Jr., and S. E. Beladi (1990), Free-Air CO<sub>2</sub> Enrichment (FACE): Analysis of gaseous dispersion arrays for the study of rising atmospheric CO<sub>2</sub> effects on vegetation, in *Green Report Series, Response of Vegetation to Carbon Dioxide*, Prog. Rep. 057, U.S. Dep. of Energy Carbon Dioxide Res. Div., U.S. Dep. of Agric. Agric. Res. Serv., Washington, D. C.
- Auerbach, D., J. Caulfield, H. Herzog, and E. Adams (1996), Environmental impacts of ocean disposal of CO<sub>2</sub>, in *Ocean Storage of CO<sub>2</sub>: Workshop 2, Environmental Impact*, edited by B. Omerod and M. Angel, pp. 41–56, Int. Energy Agency Greenhouse Gas Res. and Develop. Prog., Gloucestershire, U. K.
- Barry, J. P., K. R. Buck, C. F. Lovera, L. Kuhnz, P. J. Whaling, E. T. Peltzer, P. Walz, and P. G. Brewer (2004), Effects of direct ocean CO<sub>2</sub> injection on deep-sea meiofauna, *J. Oceanogr.*, *60*, 759–766.
- Beaulieu, S., and R. Baldwin (1998), Temporal variability in currents and the benthic boundary layer at an abyssal station off central California, *Deep Sea Res., Part II*, *45*, 587–615.
- Breaker, L. C., and W. W. Broenkow (1994), The circulation of Monterey Bay and related processes, *Oceanogr. Mar. Biol.*, *32*, 1–64.
- Brewer, P. G., G. Friederich, E. T. Peltzer, and F. M. Orr Jr. (1999), Direct experiments on the ocean disposal of fossil fuel CO<sub>2</sub>, *Science*, *284*, 943–945.
- Brewer, P. G., E. T. Peltzer, P. Walz, I. Aya, K. Yamane, R. Kokima, Y. Nakajima, N. Nakayama, P. Haugan, and T. Johannessen (2005), Deep ocean experiments with fossil fuel carbon dioxide: Creation and sensing of a controlled plume at 4 km depth, *J. Mar. Res.*, *63*, 9–33.
- Buck, K. R., J. P. Barry, and A. G. B. Simpson (2000), Monterey Bay cold seep biota: Euglenozoa with chemoautotrophic bacterial epibionts, *Eur. J. Protistol.*, *35*, 117–126.
- Caldeira, K., and M. E. Wickett (2003), Oceanography—Anthropogenic carbon and ocean pH, *Nature*, *425*, 365.
- Carman, K. R., D. Thistle, J. W. Fleegeer, and J. P. Barry (2004), The influence of introduced CO<sub>2</sub> on deep-sea metazoan meiofauna, *J. Oceanogr.*, *60*, 767–772.
- Caulfield, J. A., D. I. Auerbach, E. Adams, and H. J. Herzog (1997), Near field impacts of reduced pH from ocean CO<sub>2</sub> disposal, *Energy Convers. Manage.*, *38*, 343–348.
- deYoung, B., M. Heath, F. Werner, F. Chai, B. Megrey, and P. Monfray (2004), Challenges of modeling ocean basin ecosystems, *Science*, *304*, 1463–1466.
- Dickson, R. R., W. J. Gould, P. A. Gurbutt, and P. D. Killworth (1982), A seasonal signal in ocean currents to abyssal depths, *Nature*, *295*, 193–198.
- Feeley, R. A., C. L. Sabine, K. Lee, W. Berelson, J. Kleypas, V. J. Fabry, and F. J. Millero (2004), Impact of anthropogenic CO<sub>2</sub> on the CaCO<sub>3</sub> system in the oceans, *Science*, *305*, 362–366.
- Fer, I., and P. M. Haugan (2003), Dissolution from a liquid CO<sub>2</sub> lake disposed in the deep ocean, *Limnol. Oceanogr.*, *48*, 872–883.
- Filloux, J. H. (1971), Deep-sea tide observations from the northeastern Pacific, *Deep Sea Res. Oceanogr. Abstr.*, *18*, 275–284.
- Giere, O. (1993), *Meiobenthology: The Microscopic Fauna in Aquatic Sediments*, 328 pp., Springer, New York.
- Goffredi, S. K., J. J. Childress, F. H. Lallier, and N. T. Desaulniers (1998), How to be perfect host: CO<sub>2</sub> and HS<sup>-</sup> accumulation and H<sup>+</sup> elimination in the hydrothermal vent tube-worm *Riftia pachyptila*, in *Proceedings of the First International Symposium on Deep-Sea Hydrothermal Vent Biology*, vol. 39, pp. 297–300, Stat. Biol. de Roscoff, France.
- Gross, T. F., A. J. I. Williams, and W. D. Grant (1986), Long term in situ calculations of kinetic energy and Reynolds stress in a deep-sea boundary layer, *J. Geophys. Res.*, *91*, 8461–8469.
- Hansen, P. J., and P. K. Bjornsen (1997), Zooplankton grazing and growth: Scaling within the 2–2,000 μm body size range, *Limnol. Oceanogr.*, *42*, 687–704.
- Harvey, L. D. D. (2003), Impact of deep-ocean carbon sequestration on atmospheric CO<sub>2</sub> and on surface-water chemistry, *Geophys. Res. Lett.*, *30*(5), 1237, doi:10.1029/2002GL016224.
- Haugan, P. M., and H. Drange (1992), Sequestration of CO<sub>2</sub> in the deep ocean by shallow injection, *Nature*, *357*, 318–320.
- Herzog, H., K. Caldeira, and E. Adams (2001), Carbon sequestration via direct injection, *Encycl. Ocean Sci.*, *1*, 408–414.
- Hochachka, P. W., and G. N. Somero (2002), *Biochemical Adaptation*, 466 pp., Oxford Univ. Press, New York.
- Hoffert, M. I., Y. C. Wey, A. J. Callegari, and W. S. Broecker (1979), Atmospheric response to deep-sea injections of fossil-fuel carbon dioxide, *Clim. Change*, *2*, 53–68.
- Joos, F., G. K. Plattner, T. F. Stocker, O. Marchal, and A. Schmittner (1999), Global warming and marine carbon cycle feedbacks on future atmospheric CO<sub>2</sub>, *Science*, *284*, 464–467.
- Kennett, J. P., and B. L. Ingram (1995), A 20,000-year record of ocean circulation and climate change from the Santa Barbara Basin, *Nature*, *377*, 510–514.
- Kerr, R. A. (2001), Bush backs spending for a “global problem,” *Science*, *292*, 1978.
- Kurihara, H., S. Shimode, and Y. Shirayama (2004), Effects of elevated concentration of CO<sub>2</sub> on the life histories of marine organisms, *J. Oceanogr.*, *60*, 743–750.
- Langdon, C., W. S. Broecker, D. E. Hammond, E. Glenn, K. Fitzsimmons, S. G. Nelson, T.-H. Peng, I. Hajdas, and G. Bonani (2003), Effect of elevated CO<sub>2</sub> on the community metabolism of an experimental coral reef, *Global Biogeochem. Cycles*, *17*(1), 1011, doi:10.1029/2002GB001941.
- Leggett, J., W. J. Pepper, and R. J. Swart (1992), *Climate Change 1992: The Supplementary Report to the IPCC Scientific Assessment*, Cambridge Univ. Press, New York.
- Lien, R.-C., and M. C. Gregg (2001), Observations of turbulence in a tidal beam and across a coastal ridge, *J. Geophys. Res.*, *106*, 4575–4591.
- Marchetti, C. (1977), On geoengineering and the CO<sub>2</sub> problem, *Clim. Change*, *1*, 59–69.
- Marland, G., T. A. Boden, and R. J. Andres (2001), Global, regional, and national CO<sub>2</sub> emissions, in *Trends: A Compendium of Data on Global Change*, pp. 59–69, Carbon Dioxide Inf. Anal. Cent. Oak Ridge Natl. Lab., Oak Ridge, Tenn.
- Martin, J. H. (1990), Glacial-interglacial CO<sub>2</sub> change: The iron hypothesis, *Paleoceanography*, *5*, 1–13.
- McLeod, A. R., and S. P. Long (1999), Free-Air Carbon Dioxide Enrichment (FACE) in global change research: A review, *Adv. Ecol. Res.*, *28*, 1–56.
- Parmesan, C., and G. Yohe (2003), A globally coherent fingerprint of climate change impacts across natural systems, *Nature*, *421*, 37–42.
- Pörtner, H. O., M. Langenbuch, and B. Michaelidis (2005), Synergistic effects of temperature extremes, hypoxia, and increases in CO<sub>2</sub> on marine animals: From Earth history to global change, *J. Geophys. Res.*, doi:10.1029/2004JC002561, in press.

- Rehder, G., S. H. Kirby, W. B. Durham, L. A. Stern, E. T. Peltzer, J. Pinkston, and P. G. Brewer (2004), Dissolution rates of pure methane hydrate and carbon dioxide hydrate in under-saturated seawater at 1000 m depth, *Geochim. Cosmochim. Acta.*, *68*, 285–292.
- Riebesell, U., I. Zondervan, B. Rost, P. D. Tortell, R. E. Zeebe, and F. M. M. Morel (2000), Reduced calcification of marine plankton in response to increased atmospheric CO<sub>2</sub>, *Nature*, *407*, 364–367.
- Root, T. L., J. T. Price, K. R. Hall, S. H. Schneider, C. Rosenzweig, and J. A. Pounds (2003), Fingerprints of global warming on wild animals and plants, *Nature*, *421*, 57–60.
- Rosenfeld, L. K. (1990), Baroclinic semidiurnal tidal currents over the continental shelf off northern California, *J. Geophys. Res.*, *95*, 22,153–22,172.
- Sabine, C. L., et al. (2004), The oceanic sink for anthropogenic CO<sub>2</sub>, *Science*, *305*, 367–371.
- Seibel, B. A., and P. J. Walsh (2001), Potential impacts of CO<sub>2</sub> injection on deep-sea biota, *Science*, *294*, 319–320.
- Seibel, B., and P. Walsh (2003), Biological impacts of deep-sea carbon dioxide injection inferred from indices of physiological performance, *J. Exper. Biol.*, *206*, 641–650.
- Shirayama, Y. (1998), Biodiversity and biological impact of ocean disposal of carbon dioxide, *Waste Manage.*, *17*, 381–384.
- Someya, S., S. Bando, Y. Song, B. Chen, and M. Nishio (2004), Laser-dye imaging of the pH field in a laboratory experiment, *J. Oceanogr.*, *60*, 789–795.
- Teng, H., and A. Yamasaki (2000), Dissolution of buoyant CO<sub>2</sub> drops in a counterflow water tunnel simulating the deep ocean waters, *Energy Convers. Manage.*, *4*, 929–937.
- Thistle, D., K. R. Carman, L. Sedlacek, P. G. Brewer, J. W. Fleeger, and J. P. Barry (2005), Deep-ocean experimental tests of the sensitivity of sediment-dwelling animals to imposed CO<sub>2</sub> gradients, *Mar. Ecol. Prog. Ser.*, *289*, 1–4.

---

J. P. Barry, K. R. Buck, L. Kuhnz, C. Lovera, and P. J. Whaling, Monterey Bay Aquarium Research Institute, 7700 Sandholdt Road, Moss Landing, CA 95039, USA. (barry@mbari.org; buku@mbari.org; linda@mbari.org; lovera@mbari.org; whpa@mbari.org)